LPT

Large Petal Telescope

NG-CFHT

The Next Generation Canada-France-Hawaii Telescope

Replacement study, Final report

May 2001

TCFH-PG

Le Télescope Canada-France-Hawaii de la Prochaine Génération

Etude de remplacement, rapport final

Mai 2001

D. Burgarella (PI), K. Dohlen, M. Ferrari, F. Zamkotsian

Laboratoire d'Astrophysique de Marseille

F. Hammer, F. Rigaud, F. Sayède

Observatoire de Paris

Table of contents

1. INTRODUCTION 4

2. SCIENCE GOALS 5

2.1. FORMATION AND EVOLUTION OF GALAXIES 6
2.1.1. Galaxies 6
2.1.1.1. Quasars and Active Galactic Nuclei: Reconstruction of the density field of the intergalactic medium using absorption lines in quasars 6
2.1.1.2. Star Formation History 7
2.1.1.3. Initial Mass Function 8
2.1.1.4. Lyman α emission line and Lyman break 8
2.1.1.5. Extinction in galaxies 10
2.1.1.6. Kinematics 10
2.1.1.7. Metal Abundance 11
2.1.1.8. Morphology 11
2.1.1.9. Science Requirements for Galaxies 12
2.1.2. Stellar populations in resolved galaxies 12
2.1.2.1. Individual stars 12
2.1.2.2. Stellar clusters in external galaxies 13
2.1.2.3. Galactic structure in terms of stellar ages and abundance (in gas and stars) 14
2.1.2.4. Science Requirements for Stellar Populations in Galaxies 15
2.2. FORMATION OF STARS AND PLANETARY SYSTEMS 15
2.2.1.1. Solar system 15
2.2.1.2. Exo-Solar Systems 16
2.2.1.3. Star forming regions 17
2.2.1.4. Substellar objects 17
2.2.1.5. Science Requirements for Formation of Stars and Planetary Systems 19
2.3. REFERENCES 19

3. NG-CFHT COMPARED TO EXISTING AND PLANNED TELESCOPES 20

4. TECHNICAL PROPOSAL 21

4.1. SYSTEM STUDY 21
4.1.1. Basic concept and mission profile 21
4.1.2. Principal constituents 21
4.1.3. Interfaces 21
4.1.4. Telescope specifications 22
4.1.4.1. Functional specifications 22
4.1.4.2. Operational specifications 22
4.1.4.3. Interface specifications 22
4.1.5. Development plan 23
4.1.5.1. Adaptive structures 23
4.1.5.2. Assembly, integration and test 23
4.2. OPTICAL DESIGN 24
4.2.1. Telescope 24
4.2.1.1. Revised specifications 25
4.2.1.2. Alternative optical designs 25
4.2.1.3. The four mirror option 27
4.2.1.4. The three mirror option 28
4.2.1.5. Mirror coating 29

4.2.1.6. References....29
4.2.2. Focal plane allocation....*30*
4.3. OPTO-MECHANICAL DESIGN....31
4.3.1. Telescope:....*31*
4.3.1.1. Primary mirror segmentation: 31
4.3.1.2. Support of individual segments....33
4.3.2. Mechanical structure....*34*
4.3.2.1. Structural concept....35
4.3.2.2. Type of adaptive structure and associated study 35
4.3.2.3. The mounting 39
4.3.2.4. instrumentation supporting plate 39
4.3.3. Dome/building *41*
4.4. KEY TECHNOLOGIES 43
4.4.1. Mirror manufacturing *43*
4.4.1.1. Mirror M1 44
4.4.1.2. Mirror M2 44
4.4.1.3. Mirror M3 44
4.4.1.4. Mirror M4 44
4.4.1.5. Conclusion 44
4.4.2. Adaptive structure systems *45*
4.4.2.1. Sensing unit....45
4.4.2.2. actuator units....48
4.4.3. Adaptive optics systems....*49*
4.4.4. Micro-optics....*49*
4.4.4.1. Principle....49
4.4.4.2. Micro-Mirror Array for Multi-Object Spectroscopy 51
4.4.4.3. Micro-Deformable Mirror for Adaptive Optics Systems....52
4.4.4.4. References....54

5. MANAGEMENT....55

5.1.1. Telescope study group....*55*
5.1.1.1. Scientific consortium....55
5.1.1.2. Industrial constellation....56
5.1.2. ROM cost....*56*
5.1.3. Planning *58*

6. APPENDIX: REOSC-SAGEM REPORT 60

1. Introduction

The Canada-France-Hawaii Telescope (CFHT) saw its first light in mid 1979. It is now more than 21-year old. Thanks to the very best conditions on top of the Mauna Kea and to the evolution of the instrumentation in phase with the evolving science requirements CFHT was during these 21 years, one of the best (if not *The Best*) telescopes in the world (Fig.1). However, with its 3.6 m diameter, it has recently been bypassed by larger telescopes. Indeed, the competition with the 10-m class telescopes is now tough and the decrease of the CFHT citation fraction (Fig.2) seems to be correlated with the advent of Keck and VLT. Being aware of those potential problems, the CFHT Science Advisory Council (SAC) solicited proposals from the CFH community groups to replace the present CFHT by a world-class research facility before the end of the decade.

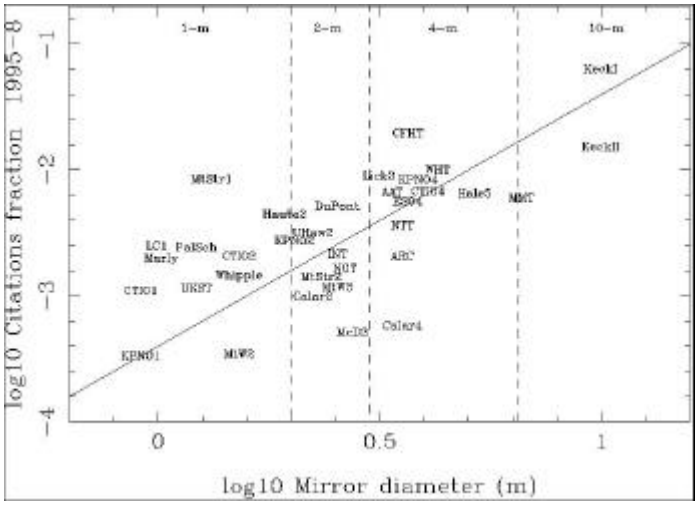

Figure 1: Citation fraction for the period 1995-1998 vs. telescope diameter of a large number of ground-based telescope. Note that CFHT is the leading 4-m telescope with respect to this criterion during this 4-yr period. Figure extracted from Benn & Sanchez (2000).

When a community is building a new telescope, this operation is often motivated by the need to observe fainter and fainter sources. We therefore try to increase the size of the primary mirror to reach farther in the universe but also fainter in the luminosity functions. But, beyond the need to collect photons, the way we are using them is more important. The development of new technologies (e.g. Wavefront Control, Adaptive Optics = AO, Micro Opto Electro Mechanical Systems = MOEMS) will certainly provide a state-of-the-art telescope coupled with state-of-the-art instruments and we believe that scientific goals in the first decade of the coming century will be more focused on physical analyses. New telescopes must be very competitive to the present-generation of 8-m telescopes. Our goal for NG-CFHT is to provide a large field of view (1 sq. degree), combined with an image quality by at least two times better than image quality currently obtained at present-day 8-m telescopes. The facility proposed here would be by several order of magnitude superior to present day 8 meter telescopes, allowing for example the study of a $z > 1$ galaxy as if it was a nearby galaxy observed with the present day CFHT.

Another parameter that we believe to be crucial is the scientific efficiency of a telescope. Beyond the increase in collecting surface, the success of a telescope is linked to the way it is used. The larger the number of astronomers who gain access to the telescope, the larger the chance to see breakthrough results coming out from this telescope. HST showed that parallel observations is scientifically rewarding. We must develop NG-CFHT to make it possible to handle this way of observing with several instruments.

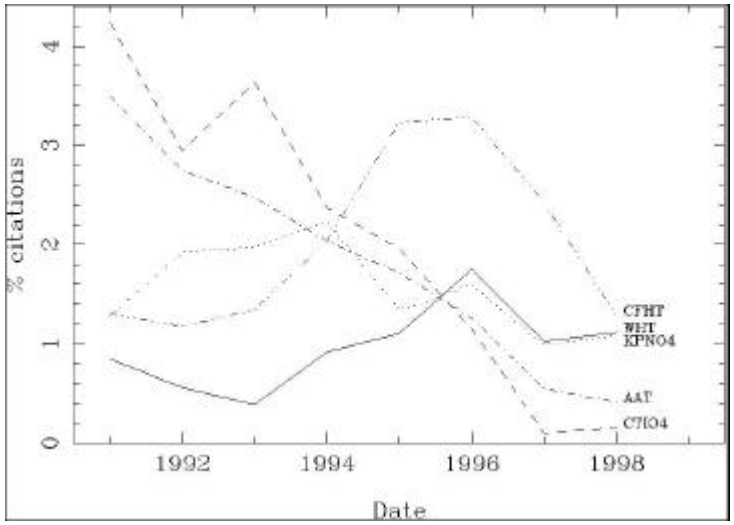

Figure 2: Citation fraction with a 3-yr running mean vs. time for a sample of five 4-m telescopes. In this figure is presented the fractions of all observational papers. Note again the leading position of CFHT in the 1994-1998 period. The decrease in the late-90s might be due to the progressive use of VLT : the commission date for first VLT instruments (ISAAC and FORS) on VLT-1 are about at the same date. Figure extracted from Benn & Sanchez (2000).

In the present report, we will present our project to build a 20 m Next Generation Canada France Hawaii Telescope (NG-CFHT). This facility would replace the present CFHT by the end of this decade.

2. Science Goals

The science objectives of most of the projects due by the end of the decade are often similar and linked in some way to NASA's Origins program. This large and ambitious program summarizes all the efforts of astronomers since the first human looked at the sky. Of course, it will benefit from a world-wide effort but no one telescope will be able to fully address the two questions raised (origins.jpl.nasa.gov /whatis/whatis.html) :

- **Where do we come from ?**
- **Are we alone ?**

Translated into an astronomical wording, the questions posed are those of the origin of galaxies - and stars within them - and the origin of planets - and life onto them. A success will only be possible through a collaborative work of all telescopes observing throughout the whole electromagnetic spectrum in space or on the ground. For this very reason and to be scientifically efficient, we must define and finely tune the characteristics of NG-CFHT in order not to overlap too much with other facilities working in the same wavelength range (for instance NGST, ground-based 10-m telescopes and other larger telescopes still to be built, very wide field-of-view telescopes such as VISTA, etc.). We have therefore started this study by trying to find the best niche(s) in the context of a telescope usable by the Canada-France-Hawaii communities. In the remainder of this section, we centre our analysis on two main themes which will be key-programs for the NG-CFHT : (1) formation and evolution of galaxies and (2) formation of planetary systems. Of course, a large number of other topics not detailed here will certainly take advantage of a 20-m telescope onto Mauna Kea.

2.1. Formation and Evolution of Galaxies

2.1.1. Galaxies

It is no surprise that understanding the formation of galaxies and their evolution up to the present day universe is within the core of most extragalactic programs. The HST and large ground-based telescope have pushed the limits of the observations to very faint objects and high spatial resolutions. The NG-CFHT Study Group defined the origin and evolution of galaxies as one of the central topics. By the end of the decade NGST and ALMA will should be able to image the first galaxies and the high-redshift universe is among the highest priority program.

CFHT (mainly from the CFRS project and follow-up programs), *HST* (essentially through the Hubble Deep Fields) and the 10-m class ground-based telescopes have allowed tremendous progresses in the last five years and we have now a rather good idea of the global star formation history over most of the universe lifetime. However, we must develop now facilities able to carry out physical studies of galaxies numerous enough to get representative samples within sub-classes (luminosity, morphological types, redshift, etc.). Indeed, a number of open questions are still waiting observational constraints :

- **Did all galaxies form through a hierarchical process (e.g. Cold Dark Matter model) where sub-clumps/disky systems formed in dark matter halos and later merged to form large galaxies, or did some of them form through a monolithic collapse?**
- **What is the evolution with time of the Hubble sequence?**
- **At which epochs was most of the stellar and metal content of galaxies formed?**

2.1.1.1. Quasars and Active Galactic Nuclei: Reconstruction of the density field of the intergalactic medium using absorption lines in quasars

A large number of absorption lines are observed in the spectrum of quasars. Through this so-called Lyα forest, we are able to get some information on neutral hydrogen in intergalactic clouds. At high redshifts ($z > 2$), the Lyα forest contains an amount of baryons very close to the predictions from the primordial nucleo-synthesis theory. Improving our knowledge of the Lyα forest is therefore a priority to understand the first phases in the formation of galaxies since it constitutes the gas reservoir out of which stars and galaxies formed.

Recently, a coherent model for the spatial distribution of intergalactic gas emerged from a confrontation of the absorption line observations and the results of N-body numerical simulations. It appeared that the spatial distribution of the clouds forming the Lyα forest follows the filamentary structure of dark matter. Nodes are likely to be the preferential galaxy formation sites (Fig.3). Studying the spatial distribution of the absorbing gas at high redshift is therefore a unique and powerful way of probing the structure of the universe, of following their cosmological evolution and to get crucial information on the formation of galaxies.

On the one side, by observing independent lines of sight, we can only have access to the 1D-structuration which mixes the local spatial and kinematical (clouds within a given halo) structures of the object (Hubble flow) and it is very difficult to disentangle these two effects. On the other side, the observations of several adjacent lines of sight allows to study the correlation of absorptions along different lines of sight. And, if the number of lines of sight is sufficient, we can characterize the 3D-structuration. Besides, inversion methods can be used to reconstruct the whole 3D-density field.

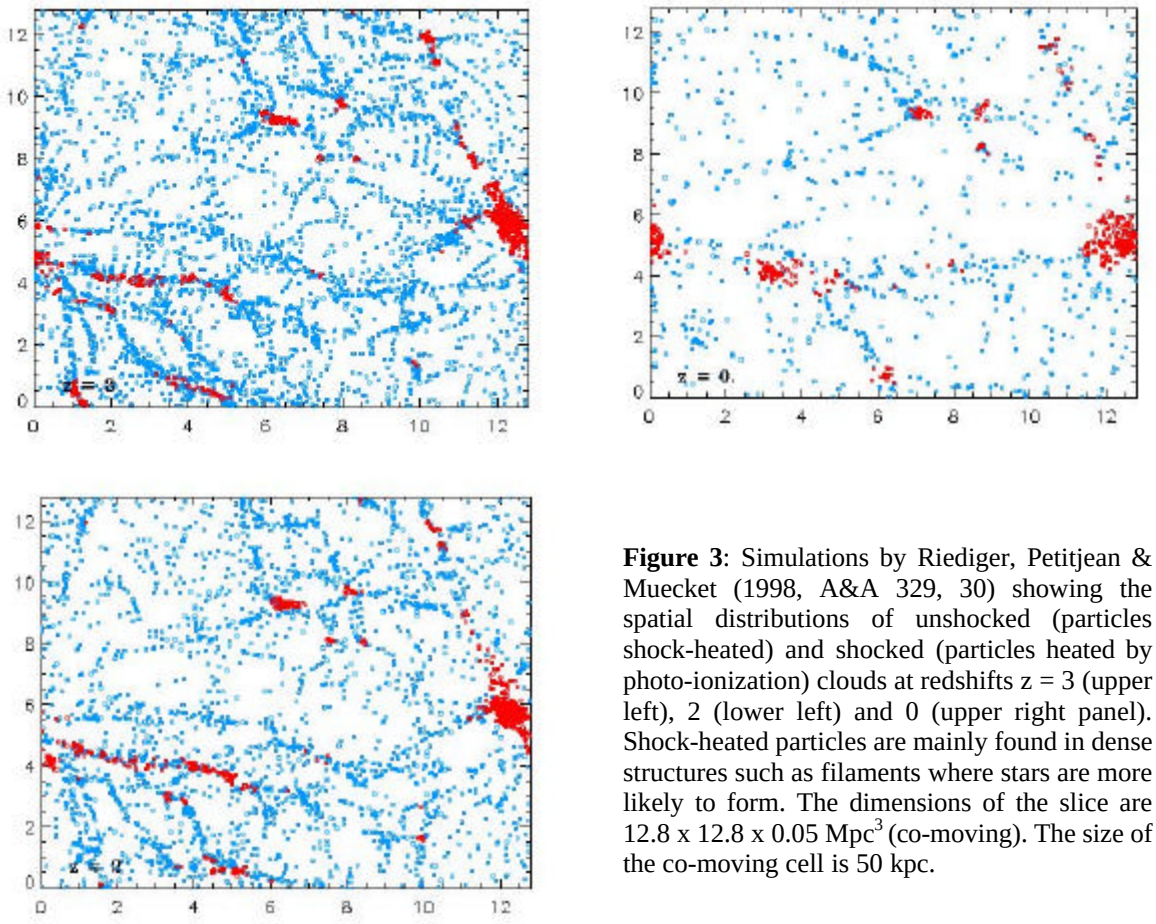

Figure 3: Simulations by Riediger, Petitjean & Muecket (1998, A&A 329, 30) showing the spatial distributions of unshocked (particles shock-heated) and shocked (particles heated by photo-ionization) clouds at redshifts z = 3 (upper left), 2 (lower left) and 0 (upper right panel). Shock-heated particles are mainly found in dense structures such as filaments where stars are more likely to form. The dimensions of the slice are 12.8 x 12.8 x 0.05 Mpc^3 (co-moving). The size of the co-moving cell is 50 kpc.

This reconstruction can only be performed if a large number of lines of sight are observed within the same field of view, with a spectral resolution of R 5000. Assuming a magnitude for the faintest accessible objects of the order of V 23, we would need exposure times of 20h or more for a 16 -m telescope. A minimum multiplexing of 10 within a field of view of 20 arcmin is necessary. We must also observe in the blue around 3500 Å for the Lyα forest but the study of C IV around 5000 Å could be carried out as well.

2.1.1.2. Star Formation History

The star formation activity is mainly traced by spectral features like the hydrogen Balmer lines and the ultraviolet continuum shortward of 2500Å. For instance, the Hα recombination line is commonly used (e.g. Kennicutt 1983) to study the Star Formation Rate (SFR) of star-forming objects at low and moderate redshift (z 0.4 in the visible and z 1.5 in the J -band). The number of photons emitted by the ionized gas of an HII region is directly proportional to the number of young stars and to the SFR over timescales of the order of 10^6 years. This is the lifetime of massive ($M > 10\ M_o$) stars emitting the Lyman continuum photons. The integrated ultraviolet light of a star forming population decreases after a single burst or reaches a plateau for a constant SFR. Under the latter assumption (reasonable to the scale of a large galaxy), the rest frame ultraviolet (shortward 2500Å) directly traces the SFR in galaxies over timescales over 100 Myrs. This is the lifetime of Intermediate-mass stars ($2 < M(M_o) < 10$). Multi-Object spectroscopy with R 1000 of a large sample of galaxies will provide the emission line diagnostics for SFR while low spectral resolution spectroscopy or imaging (R 20 – 50) will provide information on the rest-frame UV.

2.1.1.3. *Initial Mass Function*

The far UV absorption lines like Lyβ, CII or OVI (1030 -1040 Å) as well as CIV (1550Å) and SiIV (1400Å) are also very sensitive to the star formation history and Initial mass function of massive stars (Fig.4 and Leitherer et al. 1995). The Balmer lines and the rest-frame UV emission provide two independent estimates of the previous star formation events. Hence, a small variation of the current star formation rate will produce a very large effect in the ultraviolet while hardly detectable in visible rest-frame (for instance Fig.1 of Leitherer et al 1999, www.stsci.edu/science/starburst99). An interesting way to constrain the upper IMF is to compare the Hα flux related to very massive short-lived stars (M > 10 M_o) with the ultraviolet continuum dominated by intermediate stars (2 < M(M_o) < 10) (Buat et al. 1987; Glazebrook et al.1999).

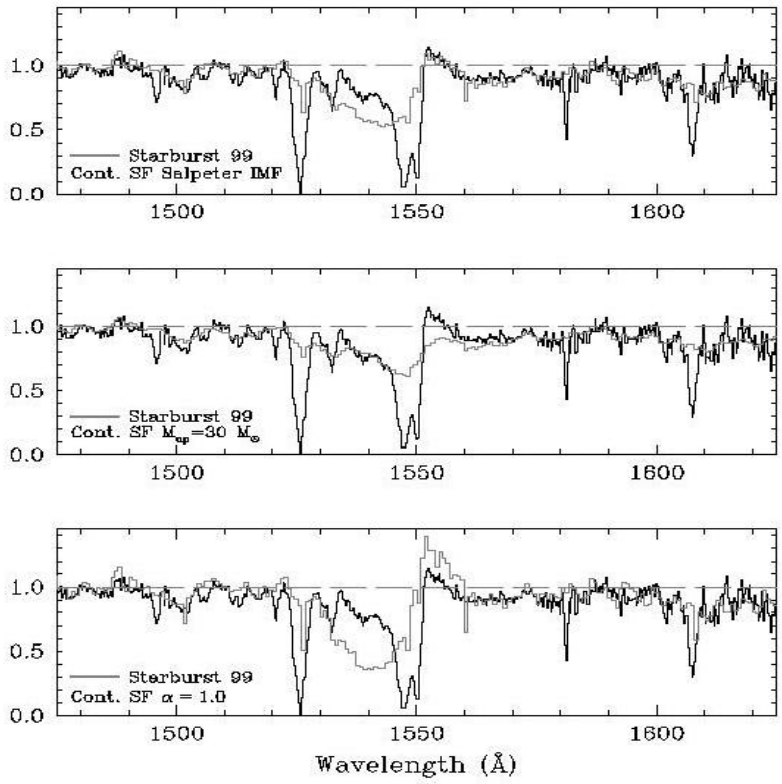

Figure 4: Comparison of the observed spectrum of the lensed galaxy at z = 2.72 MS1512-cB58 observed (black spectrum) by Pettini et al. (2000) with different spectral synthesis models (grey spectrum) from Leitherer et al. (1999). The profile of the CIV line can be decomposed into several features in absorption and emission which provide indication on the Star Formation Rate but also on the Initial Mass Function in this galaxy. It must be noted that this spectrum is the best UV-rest frame spectrum of a starburst galaxy observed thanks to the magnification (by a factor of 30 compared to a normal z 3 galaxy).

2.1.1.4. *Lyman α emission line and Lyman break*

The Lyα emission line is expected to be in principle very intense in starburst galaxies. Nevertheless, this emission has been found to be weak or absent in star-forming galaxies at low and high redshift (e.g. Hartmann et al. 1998). Very complex processes are probably at the origin of this depletion of the Lyα photons like the resonant scattering and geometrical and velocity effects in the HII regions and the HI surrounding gas (e.g. Kunth et al. 1998, Tenorio Tagle et al 1999). This might lead to asymmetric line profiles (Fig. 5). Moreover, timescale effects might also intervene, and very young starbursts (less than 10 Myr) can be found with a very large Lyman α equivalent width i.e. a very strong line and almost no underlying continuum (Stern et al. 2000). The observation of the Lyman α line in a large number of high-redshift galaxies and with a high spectral resolution will allow to test the various scenarii proposed for this line.

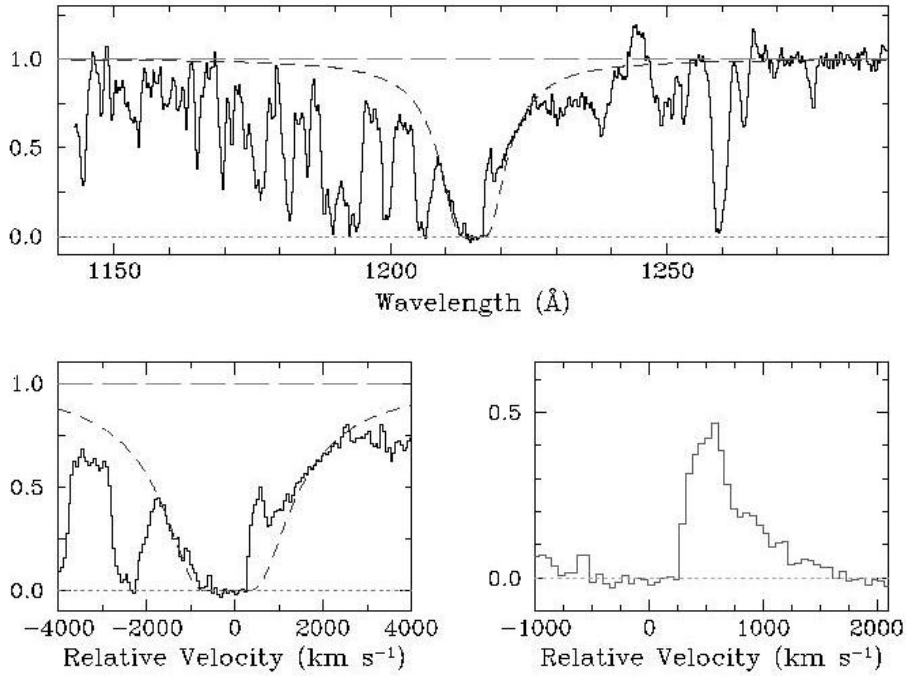

Figure. 5 :Decomposition of the Lyman α profile of the z = 2.72 galaxy MS1512-cB58 observed by Pettini et al. (2000). In the top panel, the black spectrum is the observed one and the dashed one is the theoretical absorption profile for N(HI) = 7.5 x 10^{20} $cm^{-2.}$ In the bottom left panels is presented the same line on a velocity scale. In the bottom right panel, the residual Lyman α in emission after subtraction of the absorption component. This spectrum is observed with a spectral resolution R 5000.

The Lyman break provide a powerful way of estimating the redshift, it might be used up to z 7 in the visible and up to z 12 in the J -band. With the NG-CFHT we can also hope to measure the escape fraction of the ionizing photons shortward 912Å which is an important clue to understand the ionization of the early universe (Steidel et al. 2000).

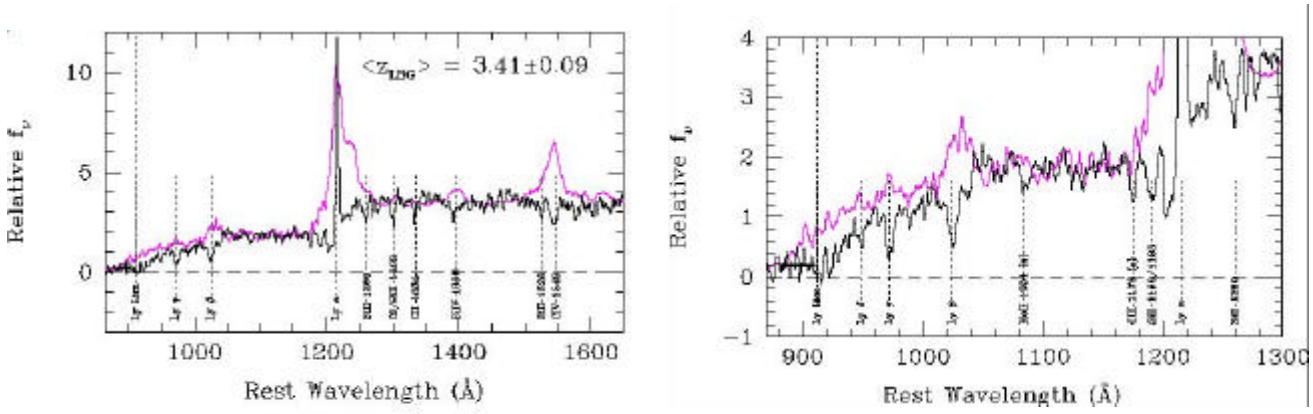

Figure. 6 : This figure presents a composite spectrum of 29 Lyman Break Galaxies at <z> = 3.40 (in black) observed by Steidel et al. (2000) along with a composite spectrum of 12 QSOs (in violet) in the redshift range 2.5 z 3.5. A significative emission over the rest -frame wavelength range 880-910 Åseems to be present in the LBG spectrum indicating that the LBGs provide more hydrogen ionising photons than QSOs at the same redshift. Carrying out these studies for galaxies at z 4 implies very good performances of NG-CFHT below 4000 Å.

2.1.1.5. Extinction in galaxies

A major limitation in using the UV emission of galaxies and the emission lines is the effects of the dust extinction which can be dramatic. The observation of several Balmer lines and in particular the Balmer decrement Hα / Hβ will allow to estimate the extinction in the lines. In starburst galaxies, the extinction in the UV continuum can be measured from the shape of the continuum (Calzetti et al. 1994). However, this relationship does not seem to hold for massive starbursts, as those detected firstly by IRAS in the nearby Universe, then those detected by ISO or SCUBA in the distant Universe. The knowledge of the star formation history of the galaxies needs data over a large range of wavelength, from the far UV to the near-infrared (rest-frame). At high redshift it corresponds to observation from visible to infra-red. The NGST will essentially observe in the near infrared, the rest-frame ultraviolet continuum ($1000 < \lambda < 2500$Å) will be redshifted in the visible for most of the observed high redshift galaxies will be observed from large ground based telescopes such as NG-CFHT if NGST has no or little visible capabilities.To estimate the extinction from the Balmer lines implies that high spectral resolution (R 2000) are needed to resolve the blend of the absorption + emission features.

2.1.1.6. Kinematics

Key questions in astrophysics are to understand the physical mechanisms which drive the galaxy and star formations. Results from the recent deep surveys (CFRS, HDF, DEEP) show that galaxies beyond z=0.5 were smaller, more irregular and showing higher star formation than present-day galaxies. IRAS, COBE and more recently ISO, have shown that nearly half of the light emitted during star formation is reprocessed by dust to IR wavelengths. The corresponding galaxies (from z=0 to z=1.5) show evidences for interactions and merging (Flores et al, 1999; Hammer et al, 2000).

The way galaxies are assembling, and how they are re-distributing their masses, velocities and angular momentum, are largely unknown. Kinematics and chemistry of galaxies should be studied at different redshifts, to determine how important the merging phenomenon is, to know the distribution of disks and spheroids at various times, and to firmly establish the evolution of the Hubble sequence. Distant galaxies are very irregular on scales smaller than 0".5. Their dynamical "sizes" are generally not larger than 50 km/s. Only 3D spectroscopy, with resolving power of a few 10 km/s and high spatial resolution, can detail their velocity fields (Fig. 6). NG-CFHT with its large field of view would allow detailed and simultaneous study of a large number of galaxies.

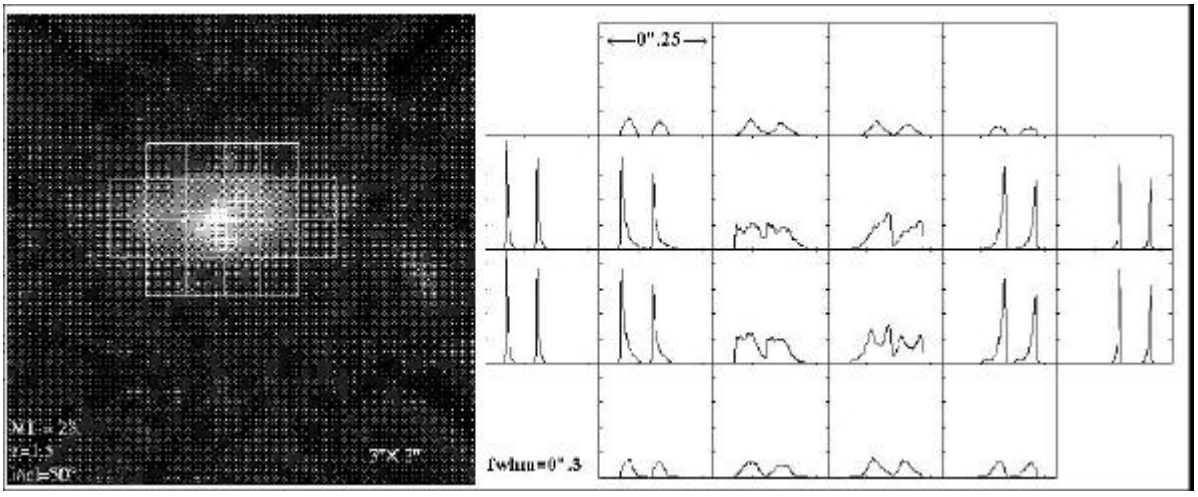

Figure. 7 : This Figure presents the simulated observation of a galaxy at a redshift z = 1.5 as it would be observed by NG-CFHT. The right panel shows the 3D-spectroscopy carried out on this galaxy. Such high spectral resolution data, providing an exceptional insight into the physics of the galaxy, is impossible today. These observations are carried out with a spectral resolution R 10000.

2.1.1.7. Metal Abundance

NG-CFHT will also be a key-facility to measure the abundance of intermediate redshift galaxies. One of the best tool to determine the oxygen abundance for instance will be to use the Edmunds & Pagel (1984, MNRAS 211, 507) R_{23} index defined by:

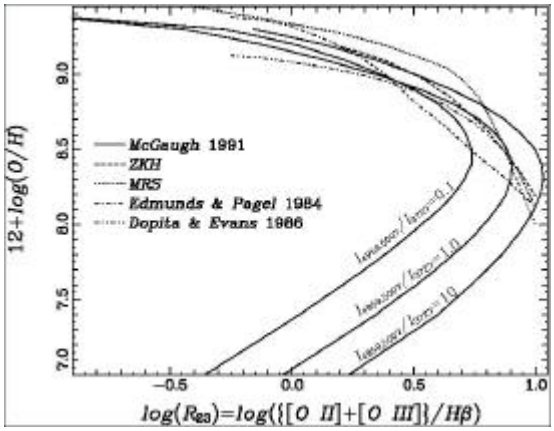

Figure. 8 : This figure from Kobulnicky et al. (1999) presents the relationship between the index R_{23} and the oxygen abundance O/H from several authors. However, the relationship is degenerated and may require some a priori knowledge of the galaxy metallicity. Indeed, at low metallicities (log Z/Z_o = -0.5 corresponds to 12 + log(O/H) 8.4) expected at high redshift, the degeneracy is raised.

$$R_{23} = ([OII]\lambda\ 3727, 3729 + [OIII]\lambda\ 4959, 5007) / H\beta$$

For metal abundance larger than 0.2 Z_o, the oxygen abundance is monotonically related to R_{23}. This technique has already been applied to high-redshift galaxies. To carry out these studies, we will also need a good sensitivity down to ground-based UV wavelengths for low-redshift galaxies.

2.1.1.8. Morphology

We cannot explain so far the origin of the Hubble sequence. Moreover, the distribution of galaxies in the Hubble sequence is apparently strongly evolving with the redshift: the frequency of spiral galaxies is decreasing at high redshift while the frequency of irregular galaxies is increasing (van den Bergh et al. 1996; Driver et al. 1998). Brinchmann et al. (1998) performed simulations and observed an apparent migration of galaxies towards later Hubble types which can be interpreted as a misclassification of galaxies by about 24 % at z 1. Bunker et al. (2000) analyze the redshift evolution of high-redshift galaxies directly from multi-wavelength data. They compare the appearance of galaxies at the same rest-frame wavelengths and find that morphological K-corrections are generally not very important. However, in the specific case of spiral galaxies, the effect is more important and when the rest-frame wavelength moves to the UV, the morphology does become more irregular. By using rest-frame ultraviolet images Burgarella et al. (2000) and Kuchinski et al. (2000) confirms this phenomenon.

As already noted before (e.g. Bohlin et al. 1991; Kuchinski et al. 2000), it seems necessary that this irregular-shifting of spiral galaxies be taken into account in morphology-sensitive works. For instance, works have been using the morphology classification of HDF galaxies to compute morphological-dependent number-counts (Abraham et al. 1996; Driver et al. 1998). The misclassification of spiral galaxies due to band-shifting is a strong bias that needs to be quantified before going on in the comparison of observations with models as underlined by Abraham et al. (1996). The effect might be negligible at redshifts below z 1 but it becomes crucial when moving at redshifts of the order of z 2. Observing UV rest-frame galaxies with high S/N ratio will play a key-role in the interpretation of future observations and in the understanding of the formation and evolution of galaxies.

2.1.1.9. Science Requirements for Galaxies

We conclude that the best niche will be to perform a physical analysis (chemistry, kinematics, morphology, stellar formation) of galaxies on a large number of objects. The field of view is a first constraint. As the limiting magnitude for point sources will be around m_{lim} = 30 for 8h-exposures. We can use the HDF to compute the total density of sources: 600 arcmin^{-2}. The number of high-redshift objects (z > 2) is lower and around 100 arcmin^{-2} in imaging. In spectroscopy, the limiting magnitude will be around m_{lim} = 24, providing about 15 galaxies arcmin^{-2} for high resolution spectroscopy (3000 < R < 20000). A wide field of view is necessary (0.5 to 1 degree) along with spectral resolutions unreachable with NGST over the whole visible / near-infrared wavelength bands are therefore needed. A number of themes also call for ground-based ultraviolet (below 4000Å) capabilities. On the other hand, we need lower spectral resolution observations to study spectral energy distributions: multi-band filters with R 20 -50 can be used in addition to more wide-band filters in imaging. In order to match the size of high-redshift, the spatial resolution must be of the order of 0.2 arcsec.

2.1.2. Stellar populations in resolved galaxies

2.1.2.1. Individual stars

Colour-magnitude diagrams remain the most secure way of analysing the nature of a composite stellar population. Individual stellar light curves (e.g. RR Lyrae, with M_V = 1, or Cepheids, brighter) give relatively direct access to distance. Red giant branch positions and slopes indicate metallicity. The main sequence turn-off and the extent of the Asymptotic Giant Branch in luminosity are measures of age. All this precious information about the stellar population is invaluable help in the understanding of the nature and evolutionary status of the target galaxy.

Determination of age and metallicity distributions are also a preliminary requirement in studies of some of the remaining most fundamental problems of stellar evolution models. One example is the "second parameter effect": the physical parameter(s) responsible for very significant changes in the morphology of horizontal branches, in old populations with similar metallicities and apparently similar ages, is (are) unknown (e.g. Sandage & Wiley 1967, van den Bergh 1967; Sweigart & Catelan 1998; Sarajedini et al. 2000).

A sensitive telescope allows to reach intrinsically fainter stars. But fainter stars are more numerous, and the confusion limit will be reached in the central regions of dense galaxies even with the highest spatial resolutions. A wide field will allow exploration of large outer regions of galaxies, where the stellar density is sufficiently low.

In practice, with a spatial resolution of 0.2'', the confusion limit for V=30 stars will be reached if more than ~ 10 stars brighter than V=30 are present within 1''. Population synthesis models show that, at distances smaller than about 100 Mpc, main sequence stars with V<< 30 are responsible for more than 90 % of the integrated light produced by all the main sequence stars present (assuming constant star formation), and that giants contribute similar amounts of optical light in addition. The limit of 10 detectable stars per square arcmin thus roughly corresponds to a surface brightness of 26.5-27 mag.arcsec^{-2} (exact values depend on the precise star formation history). In brighter regions, the depth to which photometry of individual stars will remain possible will be limited by confusion instead of the telescope's sensitivity.

At higher spatial resolution (40 mas), the confusion limit of, say, 100 stars arcsec^{-2} is reached for V=30 stars when the optical surface brightness is brighter than about 24 mag arcsec^{-2} with the same assumptions as above.

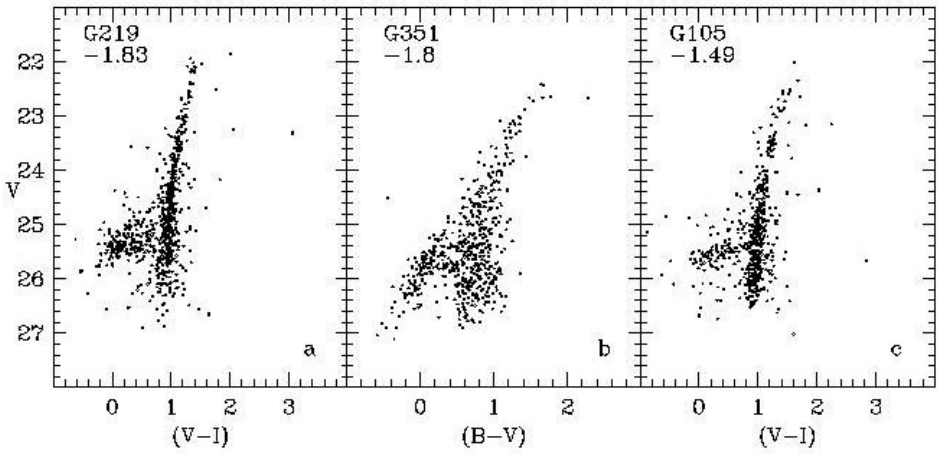

Figure 9 : The Color Magnitude Diagrams built by Fusi Pecci et al. (1996, AJ 112, 1461) on three globular clusters of M31 are examples of performances that NG-CFHT will be able to perform up to distances larger than 50 Mpc.

Stars with apparent V=30 have M_V = 1 at 60 Mpc (about 4 solar masses on the main sequence, or typical horizontal-branch stars in globular clusters), Mv = 3.5 at 6 Mpc (about 1.5 solar masses on the main sequence), Thus, horizontal branch stars can be counted out to 60 Mpc (Fig. 9) in objects with surface brightnesses fainter than 27.5 (0.2'' resolution) or than about 25 (higher resolution).

2.1.2.2. Stellar clusters in external galaxies

With a 16-m telescope the determination of cluster ages, metallicity and masses will be extended to a large number of nearby galaxies. Here we will address some specific topics related to this field. The globular clusters are considered as fossils of the galaxy formation. At present only the globular clusters around giant ellipticals have been studied with a good statistics and multiple sub-populations are frequently found which suggests that these galaxies have experienced more than one major star formation episode (Fig. 10). Nevertheless, such studies are restricted to very nearby giant ellipticals (up to the Virgo cluster) and little is known about low-luminosity field ellipticals as well as about the globular cluster systems around spiral galaxies outside the local group. Imaging capabilities down to V = 30 mag and a spectroscopic mode down to V = 25 will lead to considerable progress in this field.

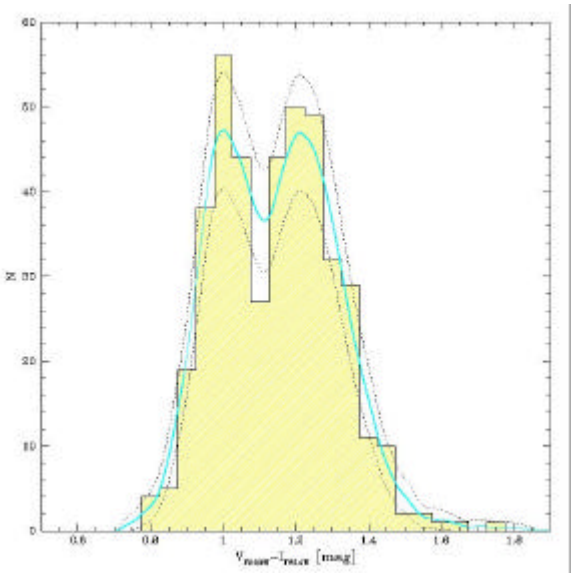

Figure 10 : Color distributions of the globular clusters around the elliptical galaxy NGC 4472 from Puzia et al. (1999, AJ 118, 777). A bimodal distribution clearly appears at the 99.99 % confidence level indicating that two globular cluster populations are present and consequently that there has been more than one stellar formation episode in this galaxy. Such studies can be carried out up to 20-30 Mpc today and may be extended up to 100 Mpc with NG-CFHT.

A typical globular cluster (Mv = -7.4) will be seen up to a distance of 300 Mpc. Nevertheless, a good sampling of the gaussian luminosity function of globular clusters needs to reach at least 1 or 2 sigma above the peak. With a peak at Mv = -7.4 and sigma=1.3 (typical values for spiral and elliptical galaxies), the luminosity function will be properly traced up to 100 Mpc. In the same way color distributions will also be obtained for such a distance.

For stellar clusters, spectroscopy is the only way to disentangle the effects of age and metallicity. Indeed, colours are affected by a degeneracy since both parameters have similar effects on them. A moderate resolution (R of some thousands) is sufficient to measure the spectral indices. It is mandatory to have a good statistics, i.e a large number of spectra of globular clusters around each galaxy (more than 100), with a limiting magnitude of 25 in the spectroscopic mode and spectral resolutions in the range 500 R 2000 and if we want to reach the peak of the luminosity function, we can observe globular cluster systems up to 30 Mpc, that is to say twice the Virgo distance.

The determination of cluster masses, once their age and metallicity are determined, gives access to the mass/light ratio and thus provides constraints on the lower part of the stellar mass function (with standard mass functions, low mass stars contribute to the mass, but insignificantly to the light). Mass determinations can be derived from velocity dispersion measurements and dynamical models. The obtention of a light profile as a constraint on the adequate dynamical model improves the precision of the estimates. Colour gradients are useful complements, as they may indicate the importance of mass segregation. A well resolved profile can be obtained for a 10pc diameter cluster with a spatial resolution of 0.2" at a distance of 1 Mpc (10 Mpc at 0.02" resolution).

2.1.2.3. Galactic structure in terms of stellar ages and abundance (in gas and stars)

The chemical and stellar evolution of galaxies is responsible for global trends such as the correlation between metallicity and luminosity, that many of the competing galaxy evolution models succeed in reproducing. Model prediction differ in more subtle points, such as the spatial variations of the abundances in gas and in stars (primary/secondary elements, products of massive/intermediate mass stars). These gradients also reflect the intimate link between the structural and the chemical evolution of a galaxy. Their study is necessary to understand the respective roles of initial collapse, of gradual gas infall, of outflows induced by massive star formation, of dynamical perturbations and of many other mixing processes. Comparison with maps of the interstellar medium, produced for instance with sub-mm or radio arrays, will help us understand the conditions under which star formation occurs, and how the processed materials are redistributed.

Colour magnitude diagram studies will remain limited to an extended Local Group. Imaging spectroscopy / spectrophotometry will remain the main tool for the systematic exploration of the structure of external galaxies.

A large telescope pushes the surface brightness limits for spectroscopic/ spectrophotometric studies of the chemistry of galaxies and their stellar populations out to larger galactic radii. Searches for the limits of stellar populations in the dark halos of galaxies can be undertaken (large fields are useful here). High sensitivity also allows us to combine spectral and spatial information in objects of low intrinsic surface brightness: known low surface brightness galaxies have typical effective surface brightnesses of 25-26 mag / sq. arcsec and 3D spectroscopy becomes possible. In irregular galaxies, clearly separated studies of the background populations underlying the patchy brighter areas become possible, allowing us to distinguish purely from spatial changes in age, extinction and chemistry.

For a typical large spiral, the I band surface brightness in the central region is around 21.6 mag per square arcsec. It decreases by about one magnitude over one disk scale length, and thus reaches about 25.5 at about 5 scale lengths of the centre. For the Milky Way (with a scale length of 3.5 kpc), this limit would be reached at a radius of 17.5 kpc.

For large galaxies, light for spectroscopy may be integrated over about one square arcsec without too much loss in spatial information. A galaxy as large as the Milky Way could be observed spectroscopically out to its outer limbs with an interesting spatial resolution at a good 100 Mpc distance.

For smaller or more distant galaxies, the telescope's spatial resolution should not be degraded. Then, the 25.5 magnitudes required for spectroscopy must be received in, typically, a 10th of a square arcsecond; limiting surface brightnesses are of the order of 23 mag/sq. arcsec. For a twin of the Milky Way, this is reached at about 5 kpc from the center.

2.1.2.4. Science Requirements for Stellar Populations in Galaxies

Stellar populations in galaxies require a high spatial resolution at 0.2 arcsec or less. The field of view must be large when we are dealing with the Milky Way or local galaxies but a few tens of arcmins is sufficient at larger distances. For very specific fields that the core of globular clusters and very dense fields, an even better spatial resolution (say 40 milliarcsecs or whatever the AO can provide) is mandatory. Spectral analysis call for high multiplexing (at least a few hundreds) and intermediate spectral resolutions (500 R 2000).

2.2. Formation of stars and planetary systems

2.2.1.1. Solar system

The discovery of a faint object (R = 22.8) in 1992 by Jewitt (1992, IAU Circular No. 5611) exhibiting a slow (3 arcsecs.hr^{-1}) motion led to the awareness of a large population of small bodies beyond Neptune at 30 - 50 AU from the sun and orbiting it. Further observations suggest that more than 100 000 (maybe millions if very small are taken into account) of such small bodies are located in a ring, which was later baptised the Kuiper Belt. The exploration of the outer Solar System has been largely driven by the desire to characterize the population of this region. The scientific interest for the Kuiper belt objects (KBO) is driven by the fact that they formed at the very beginning of the Solar system lifetime. The internal regions of the belt probably condensed very quickly to form the planets while the external regions only formed smaller objects. Consequently, the studies of small bodies in the Kuiper Belt will tell us about the accretional environment of the early Solar System. Studying their orbital distribution (which requires a field of the order of 0.5 – 1 degree in order to find them and track them) tells us about the dynamic processes which shaped our forming giant planets. Recent studies (e.g. Lynne Allen et al. 2000, astro-ph/0011037) suggest that the mean volume density of large (D > 160km KBOs is decreasing beyond ~50 AU, implying that some process or event in the history of the Solar System has truncated the distribution of 160-km planetesimals at ~50 AU. It is interesting to note that ring structures are observed around young systems where planets are still forming from circumstellar material (Fig. 11). It is probable that these ring structures are young structures analog to the Kuiper Belt in our solar system and that the central region has been partially cleared by the formation of grains into planetesimals. (Greaves et al. 1998, ApJ 506,133) Besides, it is thought that the Kuiper belt is a potential source for short-period comets. It can therefore play a role similar to the Oort cloud for long-period comets.

The discovery of the Kuiper belt, with its huge ramifications for the study of the formation of the outer Solar System, is due to the development of wide-field imaging: large areas of sky need to be imaged. CFHT led the way with the sequential deployment of several increasingly powerful large-field CCD cameras, which will finish with the implementation of MEGACAM for several years. The current extreme

over-subscription of CFH12k proves that not just solar system science benefits from wide-field imaging. Although one might argue that large-field imaging will be exhausted by 2010, it is unlikely that the entire sky will be surveyed to 25th magnitude in all filters. This is especially important in Solar System science, where the sky is continually changing due to the dynamic nature of the problem. When the CFHT closes at the end of the decade, it will leave the French community without ANY wide-field imaging capability on anything larger than a 2-meter class telescope. This seems strange given the immense effort that has been put into the development of world-class wide-field imaging capability over the last decade.

But another parameter is the faintness of the Kuiper belt objects : a deep study is necessary to assess the composition of the surface materials and to compare them with other Solar system objects. The absolute magnitude of the KBOs is directly related to their diameter. Only about 200 of them have been identified todate (Tegler & Romanishin 1999, DPS 31,2301) but to extend our quest and get a statistical view of the Kuiper Belt, we need to perform deeper observations: Gladman et al. (1998. AJ 116, 2042) deep survey found about 90 trans-Neptunian objects deg^2 brighter than 25.9.

2.2.1.2. Exo-Solar Systems

It is important to observe stellar systems at various stages of their evolution, in order to better constrain the models. For instance, the interactions between forming planets and the local zodiacal disk has little observational constraint so far, for that it needs very deep and spatially sampled observing capability. The example of iota Hor (Fig. 11), a giant planet orbiting at 1 AU from its star, is surprising: a bright dust disk is seen by adaptive optics imaging, while their coexistence with giant planets is still very controversial. It is then of importance to search for several systems having both a planet and a dust disk in order to estimate how much planets influence the dust reservoir.

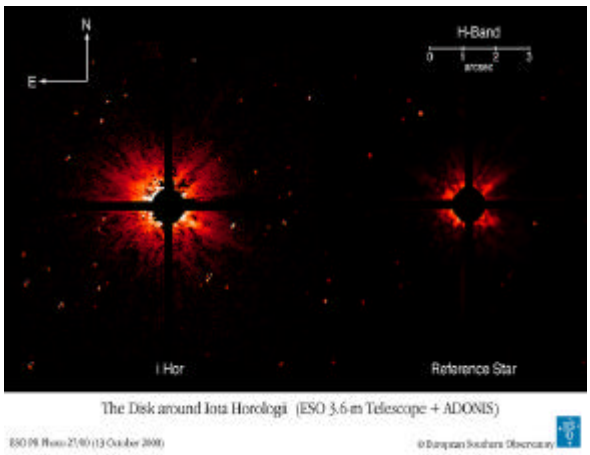

Figure 11 : Example of a dust disk detected around the star iota horologii at ESO with ADONIS. A planetary companion about twice as heavy as Jupiter was detected around this same star in an almost Earth-like orbit (ESO PR 12/99).

Also, recent observation of the planet HD209458b, a giant planet which eclipses its star every 3.5 days, allowed to probe any atmospheric signature of this far and faint object; these signature could appear as absorption features on top of the star emission. It requires both a large collecting area and a high-resolution optical and IR spectrograph. It is the only system known so far where such a demanding search is possible; it would allow to understand the nature and composition of extrasolar giant planets, without ever seen them. More candidates will be discovered by mid-term space mission, i.e. more planets passing in front of their stars on their course around it. However, it will be impossible to detect any atmosphere for these future candidates with present facilities, because their star will be too faint for 10m-class telescope. The time critical aspect of the observation of planetary eclipses would benefit a lot the simultaneous use of several instruments.
Compared with the capacity of future space-based facilities like TPF and DARWIN, the limited angular resolution of a 20 m telescope diffraction limited at 1 µm (about 20 mas) gives a reduced sample of accessible stars. Detection of planets with 1 AU orbit will only be possible for stars closer than 65 pc. The collecting power of a 20 m aperture is larger than the planned space facilities, however, and will permit

extensive studies of trajectory, albedo variations, and spectroscopy upwards of R = 100. This resolving power is sufficient for detection of life signature gases like methane and CO_2

2.2.1.3. Star forming regions

The formation of stars in our neighborhood has still many unsolved problems. The correct description of collapse mechanism has not been achieved yet, for a main reason: the pre-formed stars are embedded in opaque clouds, and their observation requires both high spatial resolution and sensitivity. Most progress in the field of pre-main-sequence stars has been made with radio or millimeter technique, which is sensitive to the gas signatures. Near-IR mapping has recently been used for creating extinction maps (Alves et al., 2000) and shows interesting perspectives for determining the physical parameters of dense cores; it requires however a large collective area (the extinguished background stars are faint) and a significant spatial sampling. Very few cores have been extensively studied so far, which limits our knowledge on the evolving processes of star formation.

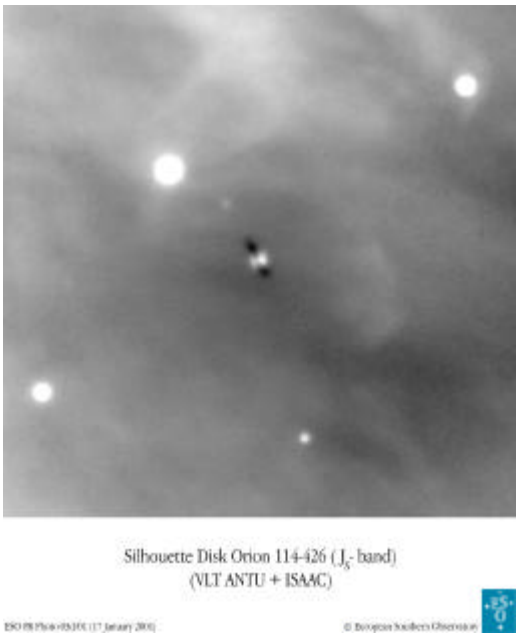

Figure 12 : A star being formed is detected here by the VLT/ISAAC near-IR spectro-imager, in Orion (Mc Caughrean et al., 2000). The edge-on disk is seen on top of the Orion diffuse emission. It contains a very young, extended proto-planetary system.

2.2.1.4. Substellar objects

The objects which mass lies in the gap between stars and planets are poorly known so far. They don't shine much light by themselves so that only a very powerful telescope is able to detect them. Brown dwarfs fall into this gap. They play a key role in the understanding of star formation processes, due to their intermediate nature. Very few such objects have been detected at present day as stellar companion, while more objects are known as "free-floating".

Brown dwarfs are brighter when they are young (Figs. 13 and 14), while they vanish while cooling down during their lifetime. The young stellar system TWA-5 of the Hyades association shows one of the few known brown dwarf companions, which spectrum could be acquired with the VLT. Optical and near-IR spectra of such objects are very rich in molecular signatures, and their effective temperature can accurately be derived.

A deep survey of nearby stars with NG-CFHT with the highest spatial resolution, would probably detect much more of such objects and thus constrain the models.

Free-floating brown dwarfs are more common (Figs. 15 and 16) ; they are isolated cool substellar objects, recognized by their red color. The dependence of the BD luminosity with respect to their age could produce an observational bias with the consequence that their density could be higher than the one measured so far. This is also suggested by the discovery of a free-floating BD in the NTT deep field, despite of the very small sky coverage.

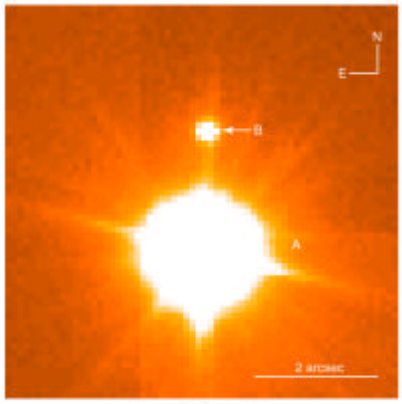

Young Brown Dwarf in TWA-5 System
(VLT KUEYEN + FORS-2)

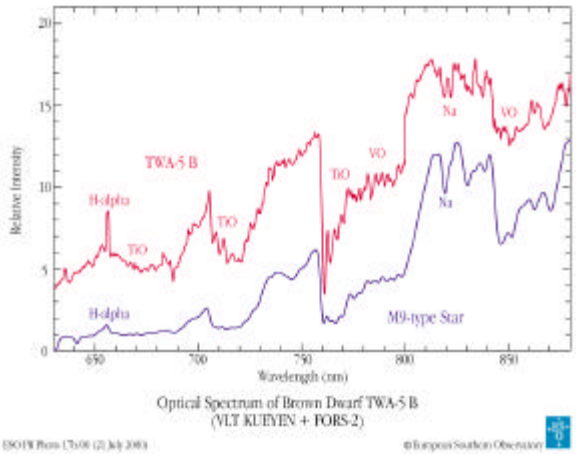

Optical Spectrum of Brown Dwarf TWA-5 B
(VLT KUEYEN + FORS-2)

Figure 13 : The young star system TWA-5 was observed here with the very best VLT image quality of 0.18" with the FORS2 instrument. A nearby companion, primarily detected by HST, is separated by 2 arcsec and shines 100 times less than the primary star; it is clearly detached on this sharp image

Figure 14 : It was then possible to obtain the first low-resolution optical spectrum from this companion (right) (Neuhauser et al., 2000), which showed the characteristic spectrum of a brown dwarf.

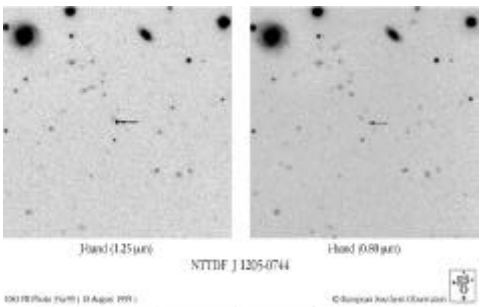

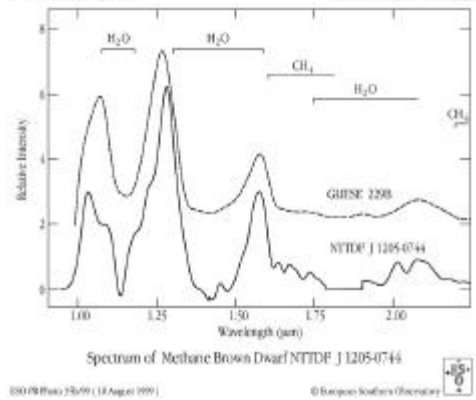

Spectrum of Methane Brown Dwarf NTTDF J 1205-0744

Figure 15 : A very red object has been detected on the NTT deep field. It is visible on the J image and absent on the optical red image.

Figure 16 : Its spectrum, acquired on the NTT and the VLT, showed the Brown Dwarf signatures. Very few such objects are known, because they are extremely faint. Their rich spectrum in the near-IR is dominated by deep and wide molecular absorption features

2.2.1.5. Science Requirements for Formation of Stars and Planetary Systems

In the first place, the search for Kuiper Belt Objects requires a field of view larger than about 0.5 degree because the density is low and these objects are moving quickly. On the other hand, reaching smaller KBOs means that NG-CFHT must detect very faint objects. To study their composition, colors might be used but low-spectral resolution spectroscopy with a moderate multiplexing (about 100) would bring better data.. Exo-Solar Systems are much more demanding : the detection of planets requires both a high spatial resolution and a high dynamics while a small field of view is sufficient. Low spectral resolution spectroscopy would also be useful to analyse the composition of the planets and their atmospheres.

2.3. References

Abraham et al. 1996 MNRAS 279, L47
Benn C.R., Sanchez S.F. 2000, astro-ph/0010304
Bohlin et al. 1991 ApJ 368,12
Brinchmann et al. 1998 499, 112
Buat et al. 1987 A&A 185,33
Bunker et al. 2000 astroph/0004348
Burgarella et al. 2001 A&A submitted
Calzetti et al. 1994 ApJ 429, 582
Driver et al. 1998 ApJ 496, 93
Flores et al. 1999 ApJ 517, 148
Glazebrook K., Blake C., Economou F. 1999, MNRAS 306, 843
Hammer et al. 2000 astroph/0011218
Hartmann L.W., Huchra J.P. Geller M. et al. 1988, ApJ 326, 101
Kennicutt R.C. 1983, ApJ 253, 72
Kennicutt, R.,C. 1983 ApJ 272, 54
Kobulnicky et al. 1999 ApJ 514, 544
Kuchinski et al. 2000 astroph/0002111
Kunth et al. 1998 A&A 334, 11
Leitherer C., Robert C., Heckman T.M. 1995, ApJS 99, 173
Leitherer et al. 1999, ApJS 123,3
Pettini M., Steidel C.C., Adlberger K.L et al. 2000, ApJ 528, 96
Riediger R., Petitjean P., Muecket J.P. 1998, A&A 329, 30
Sandage, A., \& Wiley, R., 1967, ApJ 150, 469
Sarajedini, A., Geisler, D., Schommer, R., Harding, P., 2000, AJ 120, 2437
Steidel et al. 2000 astroph/0008283
Stern et al. 2000 ApJ 537, 73
Sweigart, A.V., \& Catelan, M., 1998, ApJ 501, L63
Tenorio-tagle et al. 1999, MNRAS 309, 332
van den Bergh, S., 1967, AJ 72, 70
van den Bergh et al. 1996 AJ 112, 359

3. NG-CFHT compared to existing and planned telescopes

In order to assess the need to develop a large facility to replace the present CFHT, we need to compare the performance of the planned telescope with those presently available or already planned. A large number of 8m-10m telescopes will be available by the end of the decade (VLT, Gemini, Keck, Subaru, GTC, etc.). HST will probably be used up to ~ 2010 and although it is only a 2.4m telescope, it must be taken into account. Of course, in the Visible/NIR wavelength range, the 6m-class NGST will occupy a major place. We should also keep in mind that telescopes are often working in close cooperation and we need to keep an eye on the FIR-mm range. We assume that any 20m-30m telescope that would be built by the end of the decade will have characteristics and performances similar to ng-CFHT.

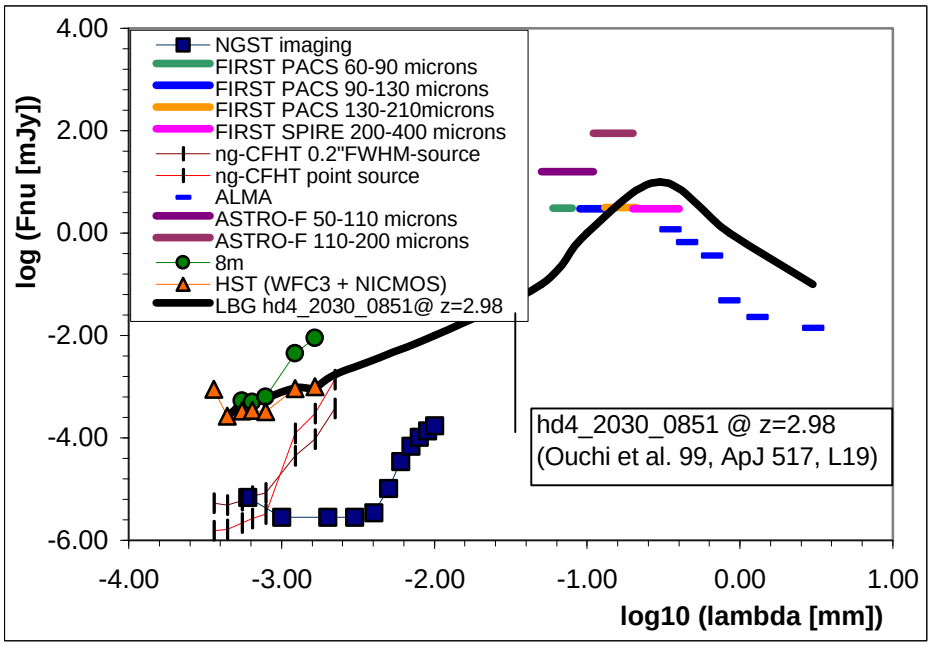

Figure 17 : This figure compares the performance of a number of telescopes in use or planned. ng-CFHT (and other 20m-class), NGST and ALMA will provide to the A&Ap community an exceptional suite. Overplotted on the figure is the SED of a z ~ 3 Lyman Break Galaxy (LBG) which could easily be observed by the three facilities.

It can be seen on Fig. 17 that ng-CFHT will be a telescope providing an ideal complement to NGST and to ALMA, in the visible wavelength range. NGST's performances will degrade below 1 μm while ng-CFHT will still be very competitive. Today telescopes (8m-class and HST) will not be able to provide such a complement. For the sake of comparing with a real object, we have superimposed the spectral energy distribution of a Lyman Break Galaxy (LBG) at z = 2.98 (Ouchi et al. 1999) with an estimated dust-corrected SFR of 60 h^{-2}_{100} Mo/yr. Fig. 17 provides a comparison for photometric observations where NGST will present an advantage in the NIR range. It must be noted, however, that if this advantage is still valid at low spectral resolution, high spectral resolution (r > 2000) observations from ground-based telescopes allow to observe through the OH lines. Moderate to high spectral resolution spectroscopy should therefore be a domain that would be favourable to ng-CFHT while high spectral resolution spectroscopy (between the OH lines) from ng-CFHT would improve the performances although the relatively high temperature of a ground-based telescope will still be bothering.

4. Technical proposal

4.1. System study

4.1.1. Basic concept and mission profile

The NG-CFHT is a 20-m class telescope to replace the existing 3.6 m telescope on the same site. The telescope concept is based on a high level of multiplexing, i.e., ability to observe numerous objects simultaneously with different instrument types. Its principal characteristics are:

- Large bandwidth, 390 nm to 2500 nm
- Large collecting area
- Large FOV (1° diameter goal)
- High angular resolution and provision for MCAO in the central part of the FOV
- Simultaneous operation of 6-8 instruments
- Optimal reuse of existing buildings

Optimal overlap between construction of the new telescope and operation of the old facility is searched in order to minimize the dead time. Its operational period is foreseen to bridge the gap between today's 10 m class telescopes and future 50-100 m telescopes, planned for 2020 or later.

4.1.2. Principal constituents

The NG-CFHT may be decomposed into the following sub systems:

- Optical system based on a four-reflection (3-4 mirrors) design and actively controlled segmented primary
- Adaptive telescope structure
- Dual-axis (alt-az) telescope pointing and tracking system
- Instrument suite
- Adaptive optics systems
- Building and its thermal control system
- Dome and its control system
- Scientific data handling, processing and storage
- Maintenance and infrastructure

4.1.3. Interfaces

Telescope interfaces to consider include:

- Building and foundations
- Remote control systems
- Data transfer and pipeline facilities
- The sky and the observational objects
- The astronomer

4.1.4. Telescope specifications

4.1.4.1. Functional specifications

FS1	Accessible FOV	< 1°
FS2	Telescope transmission, spectral range	350-500nm: >60% 500-1100nm: >80% 1100-2300nm: >80%
FS3	Telescope aperture	20m outer diameter
FS4	Time for mode changes	TBD
FS5	Pointing time	TBD
FS6	Zenithal distance	1° - 60°
FS7	Spatial resolution	• For a seeing of 0.6" and using a mag 17 (TBC) guide star separated by less than 50" (TBC) from a mag 24 object, a TBD low-order AO system shall provide 80% energy within 0.2". • The central 2' shall be diffraction limited at 1 µm to allow full MCAO correction
FS8	Observation multiplexing	> 6 (TBC) instruments working in parallel

4.1.4.2. Operational specifications

OS1	Temperature range	Operational in range: -10 to +20°C (TBC) Functionnal in range: -15 to +25°C (TBC) Survival in range: TBD
OS2	Temperature gradients	Range of gradients: -0.7 to +0.4°C/h (TBC)
OS3	Disponibility of old telescope	Until 2005
OS4	Disponibility of new telescope	First scientific light before 2010
OS5	Reliability	TBD
OS6	Maintenance	Maintenance shall be assured by the current CFHT staff level.
OS7	Lifetime	20 years
OS8	Functional duration	330 nights/year (TBC), 10 h/night (TBC), in total 66 000 hours.
OS9	Safety	TBD

4.1.4.3. Interface specifications

IS1	Re-use of old facility	Shall be optimised for minimal cost
IS2	Ground footprint	No greater than present
IS3	Mass of telescope on existing pillar	< TBD kg
IS4	Eigenfrequencies	The ensemble telescope+pillar shall have eigenfrequencies within range TBD to TBD Hz
IS5	Electrical power	< TBD Watts
IS6	Absolute pointing accuracy	1" RMS (TBC)
IS7	Tracking accuracy	0..05" RMS by the aid of guide star
IS8	Mass of dome on existing building	< TBD kg
IS9	Data pipeline capacity	TBD

4.1.5. Development plan

The development of the telescope facility is divided into five phases:

Phase A: Preliminary studies and R&D activities
Phase B: Pre-design and R&D activities
Phase C: Design
Phase D: Fabrication
Phase E: Assemblage, integration, and testing (AIT)

A tentative planning for these activities is given in the management section (sec. 5.1.3). In the present section we discuss the implementation of the phases, in particular phases A, B, and E.

Preparational conception and definition activities foreseen for phases A and B include:

- Implementation of the concept of adaptive structure in the context of a large astronomical telescope
- Conception of a 20 m segmented primary mirror with active control of segment shape and inter-segment phasing
- Fabrication procedure for large concave secondary
- Thermal studies of structure and dome

4.1.5.1. Adaptive structures

Apart from the obvious difficulties involved in the fabrication of the optical surfaces for a versatile 20 m telescope, a major component of the proposed concept is the use of an adaptive structure. Adaptive structures consist of dimensional sensors and actuators operating in closed loops. Acting upon the structure carrying the optical surfaces, perfect alignment of the telescope is continuously ensured. The use of such structures optimizes the ratio mass/performance by including structural sensors and actuators which, when operated in closed loop, assures constant dimensions of the structure in the presence of varying external perturbations (gravity vector, thermal variations, wind loading (TBC), etc), see Sec. 4.3.2 and 4.4.2. System level analysis in phase A/B must be performed in order to identify and evaluate the external factors involved and to establish operational frequencies, adjustment ranges, and required precisions, both for the actuation and for the measurements. On the basis of such studies, optimal structural parameters (stiffness, mass, etc) can be established and the gain with respect to a passive structure can be evaluated.

4.1.5.2. Assembly, integration and test

This concerns assembly and testing of telescope sub systems as well as final integration and testing of the entire telescope. Typically, the following structural tests should be applied:

- Static tests under load to determine residual deformations
- Thermo elastic tests to characterize thermal deformations
- Vibration tests to determine vibrational modes and their propagation in the structure
- Functional tests
- Optical performance

The large dimensions and high precisions involved render these tasks heavy and delicate. The use of adaptive structures can relax the assembly tolerances by at least an order of magnitude as long as these requirements are taken into account in the design of theses systems so that the added adjustment range is provided.

Optical performance measurements must be based upon the analysis of astronomical objects by the aid of wavefront sensors (WFS). Its use during the integration permits the definition of an absolute zero for the adaptive structure. The strategy for the use of WFS during telescope operation must be defined. Permanent monitoring of the telescope optical quality as in VLT is surely necessary, at least for the primary mirror shape control.

4.2. Optical design

4.2.1. Telescope

Our original proposal consisted of a fast 16 m Ritchey-Chretien telescope with a primary at F/1 and a Cassegrain focus at F/3 provided by a 5 m secondary (Fig.12). The circular primary consisted of four or six 6-8 m segments. With a focal length of 48 m, the 4 deg FOV covered 3 m, fitting within the secondary obstruction. The focal surface was curved and poorly corrected beyond some fraction of a degree, but with local active corrector optics, aberrations could be eliminated within instrument sub-fields, offering diffraction limited operation at any point in the FOV.

The focal surface was divided into four concentric zones:

Zone 1: In the inner disc of diameter 2', diffraction limited at 1 micron.
Zone 2: Out to a diameter of 11', seeing limited with geometrical spots smaller than 0.3"
Zone 3: Out to a diameter of 30', astigmatism only considerable aberration
Zone 4: Out to a diameter of 4°, complex combination of aberrations.

The focal ratio of F/3 provided a plate scale of 0.23mm/arcsec. For NGST-type NIR detectors with 27µm pitch paving the Zone 2 in a Megacam manner, this provided a sampling of 0.12" per pixel, requiring a 5.7K square array.

Although the concept of local correction has been proven by optical modelling, it has only been found possible for very small sub-fields (few arcseconds). Correction over arcminute-sized sub-fields would require exceedingly large and complex optics. The outer focal plane zones are therefore limited to the study of compact objects, either with a seeing limited single pixel approach (Giraffe), seeing limited or low-order AO corrected multi-pixel approach (Giraffe, Falcon), or using classical, single-conjugate AO.

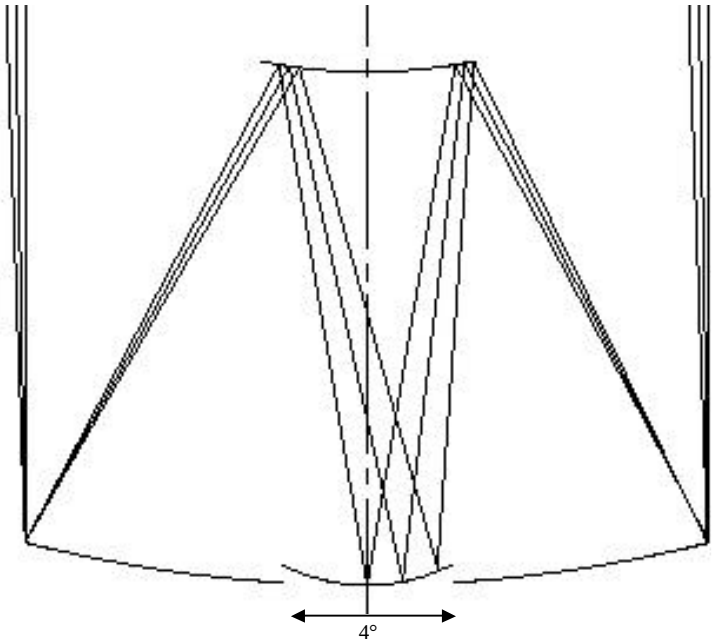

Figure 12. Preliminary optical design of the large FOV versatile NG-CFHT concept.

4.2.1.1. Revised specifications

As seen in the scientific discussion above, the merit of a 4° FOV under these conditions are not obvious, and it has been decided to search for more complex optical designs providing better performance over FOV diameter greater than 0.5° with a goal of 1°. A set of baseline zones within this FOV have been defined:

Zone 1, diameter 2': Diffraction limited at 1 micron.
Zone 2, diameter 10': Sub-seeing limited, better than 0.2"
Zone 3, diameter 30' - 1°: Median-seeing limited, better than 0.6"

Also, a focal ratio in the range F/5-10 would be preferable in order to facilitate design of instruments. This eliminates the possibility to pave the focal plane directly, but it was felt that such Megacam approach should be reserved for dedicated telescopes, and that the NG-CFHT should favour a more analytical, multi-instrument approach. Large FOV imaging would therefore require focal reduction as in VIRMOS-style instruments, providing very fast camera optics with F/1 - F/3. A telescope focal ratio of F/7.5 has been taken as a good compromise.

Telescope size has been considerably discussed, in particular during the Victoria meeting in April 2001. Greg Fahlman then gave a more relaxed view on the requirements given in the Mauna Kea Master plan, allowing somewhat larger structures to be conceived. It was agreed to aim for a 20 m telescope.

Baseline telescope parameters and platescale.

Entrance pupil diameter	20 m
Focal ratio	F/7.5
Focal length	150 m
Plate scale	2.6 m/deg 44 mm/arcmin 0.7 mm/arcsec 1.4 arcsec/mm

The telescope should have a fast primary for telescope compactness, an important mechanical design parameter. Obtaining a large well-corrected FOV becomes difficult for primaries much faster than F/1, however. Another consideration to take into account is fabrication facilities. The existing REOSC tower allows testing of mirrors with curvatures up to 35m (see appended report), indicating a primary focal ratio of 0.88 for a 20m primary. They are willing to do necessary changes and we are currently analysing this with them in terms of possibilities and relative costs.

M1 and M3 should lie in the same plane to benefit from the same support structure, and the focal plane should be located 2 m below the primary for accessibility.

4.2.1.2. Alternative optical designs

The revised telescope specifications eliminate classical two-mirror (Richey-Chretien) telescope designs which only correct spherical aberration and coma, leaving astigmatism uncorrected. According to the Schwarzschild principle (Wilson, 1996), three aspheric mirrors are necessary in order to correct all three third-order aberrations. Wilson provides a thorough review of telescope designs with three or more mirrors, in both single axis (Cassegrain) and double axis (Nasmyth) configurations. We consider the advantages of the single-axis configuration to be prevailing (compactness of opto-mechanical design, accessibility of focal plane, limited variability of gravity vector) and have therefore concentrated on this class of designs.

The simplest three-mirror design, as proposed by Rumsey (1969), see Fig. 13(a), has the tertiary in the plane of the primary and the final focal plane behind the secondary mirror. This design is impractical for

many reasons in the context of a multi-purpose telescope (focal plane accessibility, instrument seeing, etc), and we have not investigated it further.

The more classical Cassegrain position behind the primary may be obtained by adding a fourth mirror between the primary and the secondary, Fig 13(b). When the primary is aspheric, this mirror may be spherical or even flat, reducing constraints on alignment and difficulty of fabrication. However, it is close to an image of the telescope pupil and may therefore be used to correct the spherical aberration of a spherical primary mirror (Robb 1979). Wilson & Delabre (1995) claim excellent image quality over a 1.5° FOV in a similar design for a 4m telescope with a spherical primary. The size of the corrected FOV reduces as the primary gets faster and the ratio between M1 and M4 diameter gets larger. The trade-off between fabrication of an aspheric primary versus a smaller but highly aspheric quarternary is not obvious however, see the Reosc report, since the required null lens is the same in both cases.

A third design option, due to Korsch (Wilson 1996) consists of using the secondary mirror as quarternary, eliminating the need for a fourth mirror, see Fig 13(c). This very elegant solution has the obvious advantage of reduced mechanical complexity and limited number of alignment parameters. Since M1 and M3 are in the same plane, they may be mounted in a common structure, reducing, if not eliminating, their relative displacements. The positioning of the secondary remains the only critical item; one may indeed predict that its alignment sensitivity doubles because it is used twice. An opto-mechanical trade-off is required.

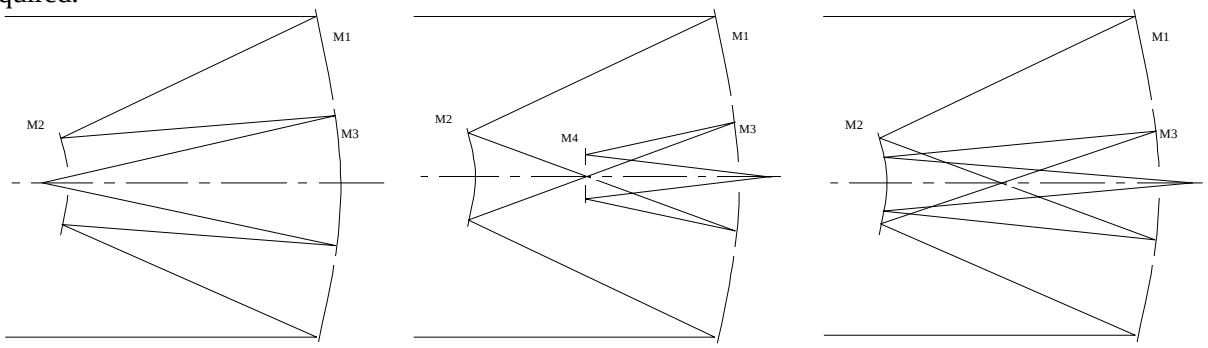

Figure 13. Basic options for single-axis telescope designs using three aspherics: Rumsey (a), Robb (b), Korsch (c).

4.2.1.3. The four mirror option

A design based on the four-mirror Robb concept has been created for a final focal ratio F/5, see Figure 14. Further investigations are required in order to transform it into F/7.5. The design has an aspheric primary and a flat quarternary, but since M4 is very close to the pupil, it should be possible to obtain similar field characteristics with a spherical primary and an aspherical, Schmidt-plate M4.

Image quality is illustrated in Fig. 15. The design is diffraction limited at 1 µm out to a diameter of about 15', and the geometrical spots are smaller than 0.2" out to a diameter of about 50'. Exceeding 1°, image quality degrades rapidly and the size of M3 and the central obscuration become prohibitive.

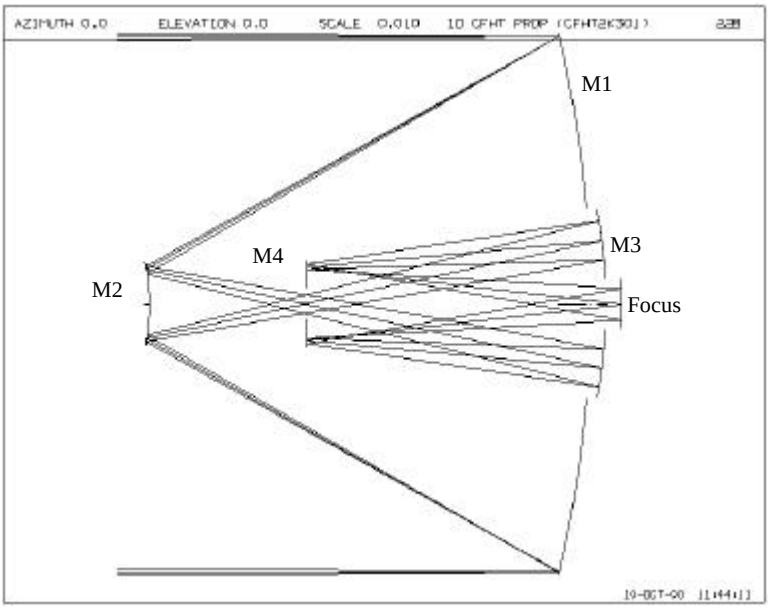

Figure 14. Beam diagram showing rim rays for an axial object and objects at ±22' (FOV = 0.75°).

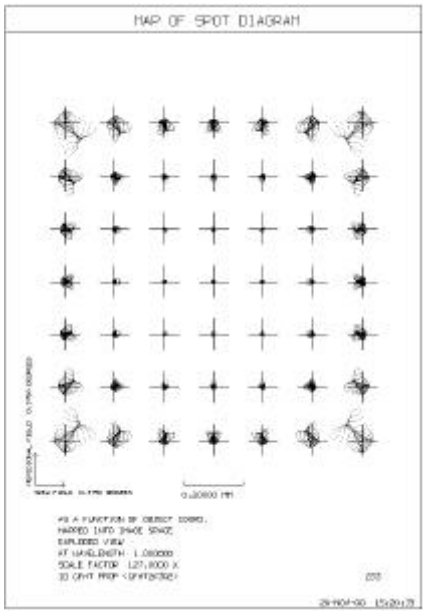

Figure 15. Spot diagrams for the four-mirror, F/5 design. The FOV shown has a 1° diagonal, crosses are 100 µm (0.27") wide.

Linear central obscuration for an axial object is about 30%, corresponding to 9% of the pupil area. This increases towards the edge of the field, mainly due to beam "walk" on M4, and at 30' from the axis, the areal obscuration reaches 19%.

Scaled to 20m diameter, this design is characterised as follows:

M1: 20 m diameter with a central hole of about 7 m. With a 40m radius of curvature, the primary focal ratio is 1. Its aspheric shape is nearly parabolic.

M2: 3 m convex hyperboloid. From a fabrication point of view, this is a great improvement with respect to the original R-C proposal, for which the secondary was a 5m convex.

M3: 7 m prolate ellipsoid with a 500 mm central hole to access the focal plane.

M4: 3.3 m flat mirror with a 1 m central hole.

The focal plane has a curvature of 16m, curved towards M2. With a final focal ratio of F/5, the defocus at the edge of a 3' sub-field is 40µm, corresponding to a geometrical defocus spot diameter less than 10µm (0.025"). Such a field curvature therefore appears acceptable.

The use of a spherical primary mirror in this design hs been investigated, but it has been found that this sets a severe limit on the size of the FOV. The main parameters in this context are relative size of M1 and M4, and primary mirror focal ratio. Since structural concerns tend to pull towards fast primary and small M2/M4 mirrors, and since there is no decisive advantage in a spherical primary from an optical fabrication point of view, this option is no longer persued for this telescope.

4.2.1.4. The three mirror option

A three-mirror Korsch design has been created for a final focal ratio F/7.5, see Figure 16. Due to its double use of M2, this design is highly constrained and offers little room for geometrical variations. An important result of this is a large (4.9 m) secondary mirror and a fairly curved focal plane. This situation may be improved at the price of an increased M1-M2 separation and larger M3 diameter. The optimal design must be determined by a thorough opto-mechanical trade-off study.

Image quality is illustrated in Fig. 17. The design is diffraction limited at 1 µm out to a diameter of about 30', and the geometrical spots are smaller than 0.2" over the entire 1° FOV. Exceeding 1 degree, image quality degrades rapidly and the size of M3 and the central obscuration become prohibitive.

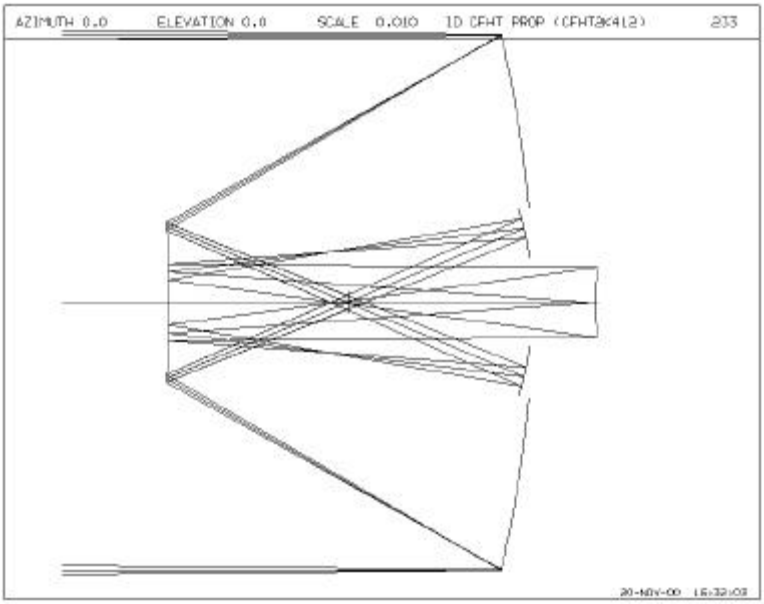

Figure 16. Beam diagram showing rim rays for an axial object and objects at ±22' (FOV = 0.75°).

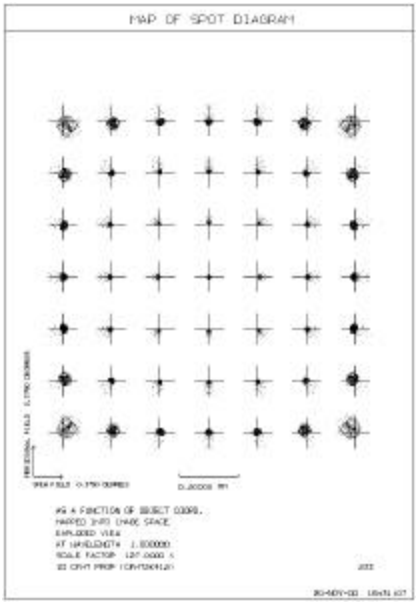

Figure 17. Spot diagrams for the three-mirror, F/7.5 design. The FOV shown has a 1° diagonal, crosses are 100 µm (0.18") wide.

Linear central obscuration for an axial object is about 50%, corresponding to 25% of the pupil area. Further optimization may reduce this somewhat at the price of a larger tertiary mirror.

Scaled to 20m diameter, this design is characterised as follows:

M1: 20 m diameter with a central hole of about 7 m. Primary focal ratio is 1. Its aspheric shape is ellipsoidal with a conic constant of -0.8.

M2: 6.1 m convex hyperboloid.

M3: 6.5 m diameter prolate ellipsoid (cc = -0.5) with a 2.9 m central hole to access the focal plane.

The focal plane has a curvature of 5.8 m, curved away from M2. The defocus at the edge of a 3' sub-field is 1 mm, corresponding to a geometrical defocus spot diameter less than 130µm (0.23"). It should be possible to absorb this amount of field curvature in the instrument optics.

4.2.1.5. Mirror coating

Investigations made for the Gemini project identifies protected silver as the most promising coating for 8m telescopes (Wilson 1999, p. 434). As seen in Figure 18, silver is substantially better than aluminium over the entire visible band and well into the infrared. Below 390nm, the reflectivity of standard protective silver quickly drops, however. Enhanced silver coatings pushing this edge down to below 300 nm exists, but it is not clear whether such coatings are equally performant at longer wavelengths and sufficiently resistant. The table gives telescope efficiency assuming four reflections off protected silver mirrors.

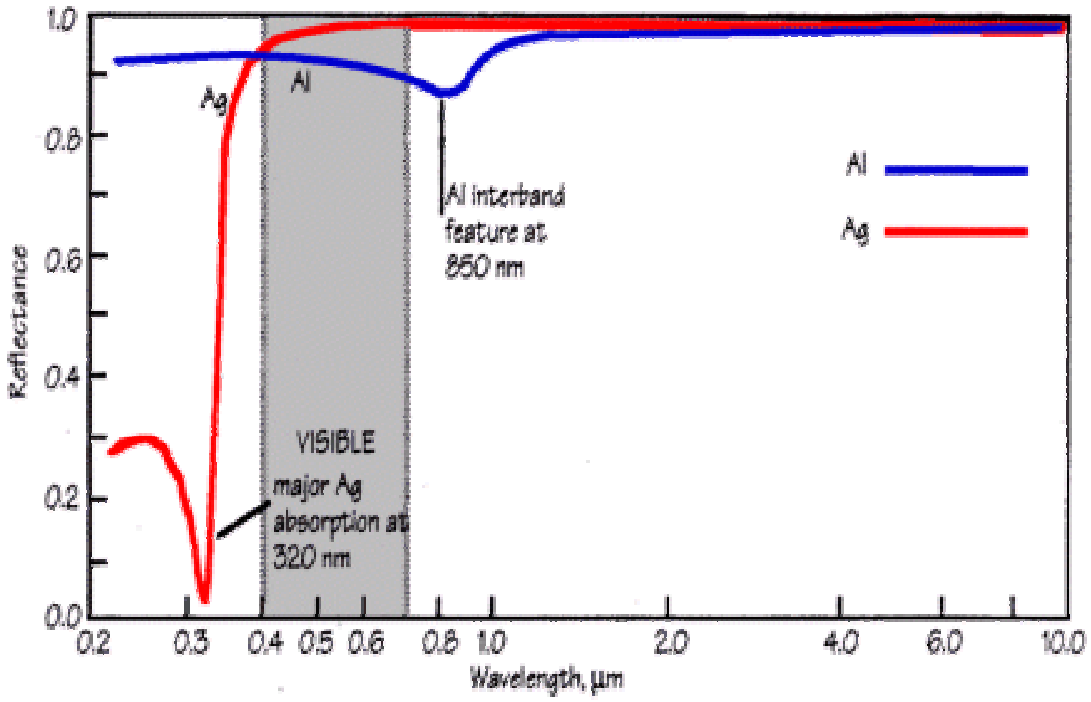

Figure 18. Comparison of silver and aluminium mirror coatings.

Telescope efficiency with protected silver coating.

Wavelength	**390**	**500**	**1000**	**2500**
Surface reflectivity	90%	98%	99%	99%
Telescope efficiency	65%	92%	96%	96%

4.2.1.6. References

P. N., Robb, JOSA 69, 1439 (1979).

N. J. Rumsey, "A compact three-reflection astronomical camera", in Optical Instruments and Techniques, ICO 8th meeting, Ed.: Home Dickson, Oriel Press, Newcastle (1969).

R. N. Wilson, Reflecting telescope optics I, Springer Verlag, Heidelberg (1996).

R. N. Wilson, Reflecting telescope optics II, Springer Verlag, Heidelberg (1999).

Wilson, Delabre, "New optical solutions for very large telescopes using a spherical primary," Astron. Astrophys. 294, 322-338 (1995).

4.2.2. Focal plane allocation

In the case of the three-mirror telescope, the 1° field of view may be divided into two areas, a central 30' zone, diffraction limited at 1 µm wavelength, and the surrounding ring with a maximal 0.18" residual optical aberration.

We allocate nine instrumental zones in the focal plane.

- A 10' central zone will be reserved for high spatial resolution instruments with advanced Adaptive Optics (AO) systems. Two types of AO systems are foreseen, a low-order correction AO on contiguous 3'x3' fields for a 0.2" spatial resolution and/or an MCAO on contiguous 1.5'x1.5' for diffraction limited operation.

- Eight sectors are located around the central zone allowing simultaneous observations using separate instruments. We have identified six observational modes, each corresponding to an "instrument class" (Fig. 19):

  - Wide Field mode (15 to 20' squares) for seeing limited observations, imaging, low-medium resolution spectroscopy (Megacam, Virmos)
  - Medium field mode (3'x3') with low-order AO correction for a 0.2" spatial resolution, imaging, low-medium resolution spectroscopy.
  - MCAO mode, 1' field in the diffraction limited area of the focal plane.
  - Classical AO mode for diffraction limited operation over a few arcsec field of view.
  - Fiber-coupled multi-object mode for high-resolution spectroscopy and integral field spectroscopy, >100 buttons in a field of view of 20'x20'.
  - Seeing limited, single or multiple fibers
  - ~0.2" spatial resolution with integrated low-order AO correction
  - Visitor mode (coronography, AO,…).

These modes are replicable and could be implemented in one or more sectors, permitting a high degree of flexibility and versatility.

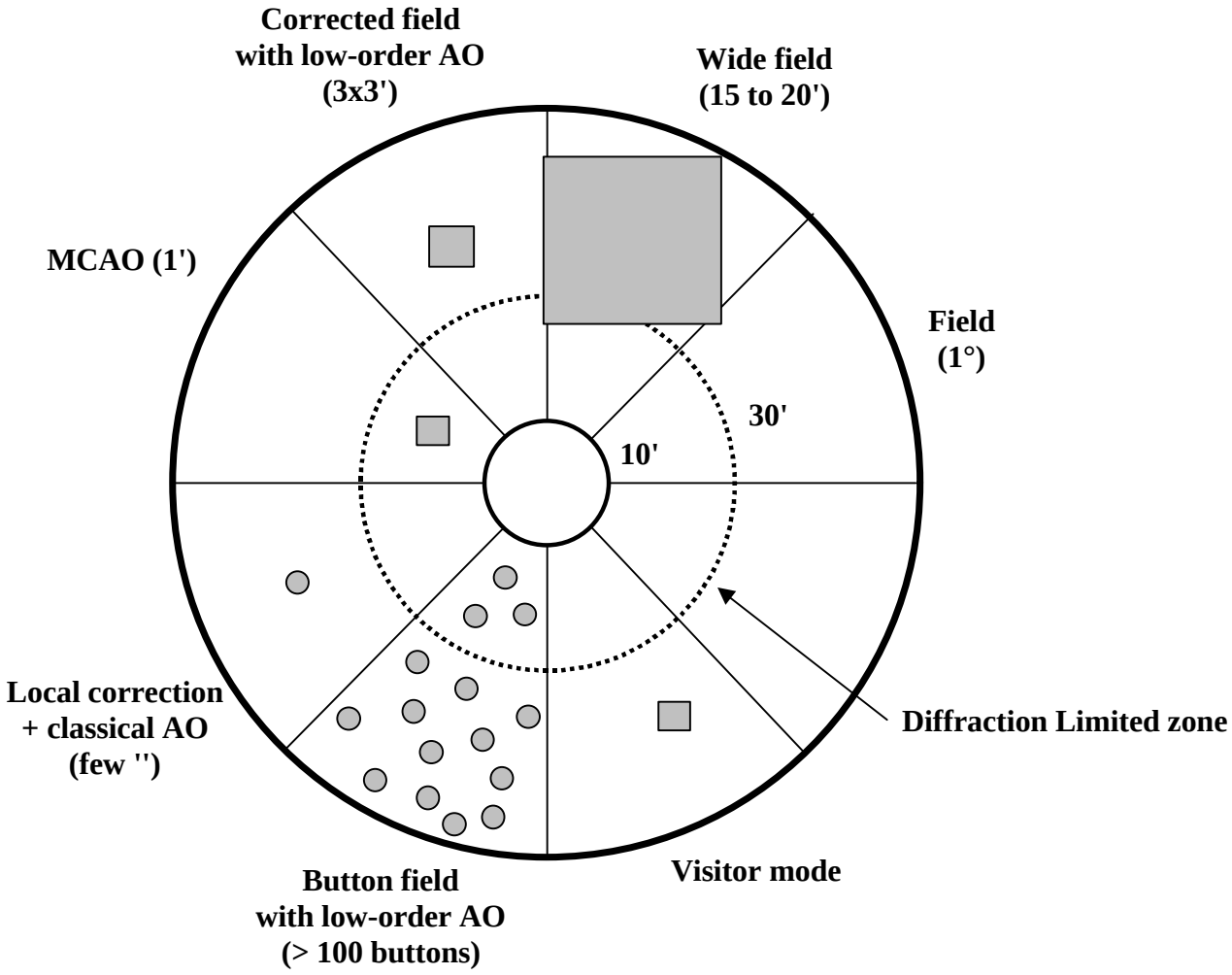

Figure 19. Focal plane allocation scheme.

4.3. Opto-mechanical design

4.3.1. Telescope:

4.3.1.1. Primary mirror segmentation:

The proposed design includes the two major concepts proven during the last decade, segmentation and active optics, in a way that allows to combine advantages and minimize drawbacks of each approach.

Active optics on large segments will permit 1) to use computer controlled thin meniscus mirrors (VLT/Gemini type) and reduce overall primary mass, 2) to relax fabrication tolerances and thus reduce cost. Large-segment segmentation as we propose will allow an important step forward in collecting power with use of existing 8-m class manufacturing tools. Also, the use of identical segments permits cost savings.

In the proposed 20 m designs, the primary mirror is composed of 8 off-axis aspheric 8-m class mirrors (Fig. 20). Compared with the use of a large number of 2-m passive segments, the use of large active segments has some advantages:

- With a limited number of segments the problem of surface discontinuities between segments and hence of scattered light is reduced. The phasing algorithm, using position sensors and other techniques, is also less complex.

- For 2-m size passive segments tight tolerances are imposed on the surface figure, and this leads to severe material selection and polishing tolerances. For the 8-m class active segments, figure errors can to a large extent be corrected by the support system, and these tolerances can be relaxed.

A preliminary alignment and phasing procedure has been established. This procedure is tentative and a complete evaluation has to be performed.

- The secondary mirror is taken as the optical axis reference.
- The six petals/segments are centred and aligned relatively to the secondary axis by using adaptive telescope structure and tip-tilt control of individual segments. This procedure is automatic and referenced to the optimal alignment defined during the telescope integration and test phase.
- The shape of individual segments is controlled using a Shack-Hartmann (SH) sensor.
- Finally, co-phasing of the segments is achieved by piston correction of individual segments and a TBD phasing sensor.

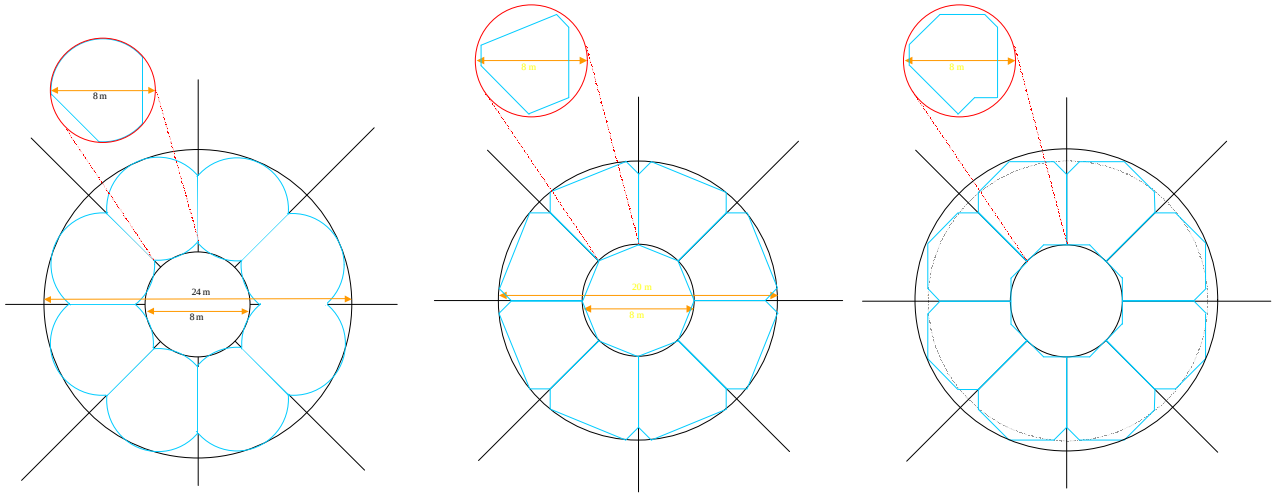

(a) (b) (c)

Figure 20. Three different segmentation concepts for a 20-m class large-petal telescope using 8 x 8m segments. (a): Optimal use of 8m, quasi-circular segments. The outer pupil diameter is 24m and the collecting area is estimated to 350 m^2. (b): 8 m-sized modified hexagons. An excellent aperture fill factor is achieved, but the hexagonal geometry produces a large number of diffraction directions, hence complex instantaneous PSFs. (c): 8 m-sized modified octogons. Ensuring all edges to be aligned along a multiple of 45°, this option restricts the number of diffraction directions to four (8-armed stars).

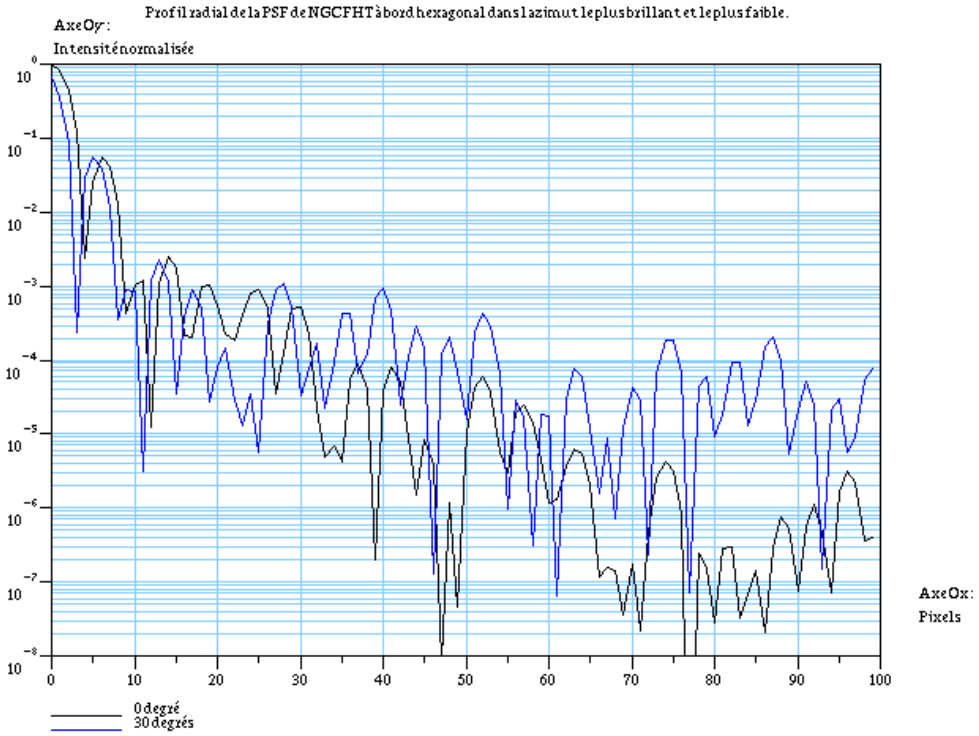

Figure 21 : Radial PSF profiles for the case of a six-petal modified hexagon design in the faintest and brightest azimuths. It suggests a very good spatial resolution.

4.3.1.2. Support of individual segments

The surface of each individual segment will be computer controlled using a SH sensor and a large number of actuators (100-200) as it is done in current 8-m class telescopes. The system complexity at operational and maintenance levels of such active systems and the sensibility to frequencies higher than the control-loop, are well identified and managed in present-generation large telescopes. The number of segments used in NG-CFHT will increase this system complexity but by less than one order of magnitude. As the six segments are identical, their support systems will also be identical, a single S-H sensor will measure the entire pupil simultaneously.

Concerning tip-tilt control of individual segments, a support concept using three position controlled actuators in addition to the active figuring system has been studied. An alternative solution would be to correct tip-tilt of individual segments by moving the associated cell, but the mass to displace is then important and can generate other flexions and misalignments of the structure. Further evaluation and trade-offs will be done in the next phase. Preliminary finite-element analysis has been done to optimize the position of the three support points for minimal deflection (Fig. 21).

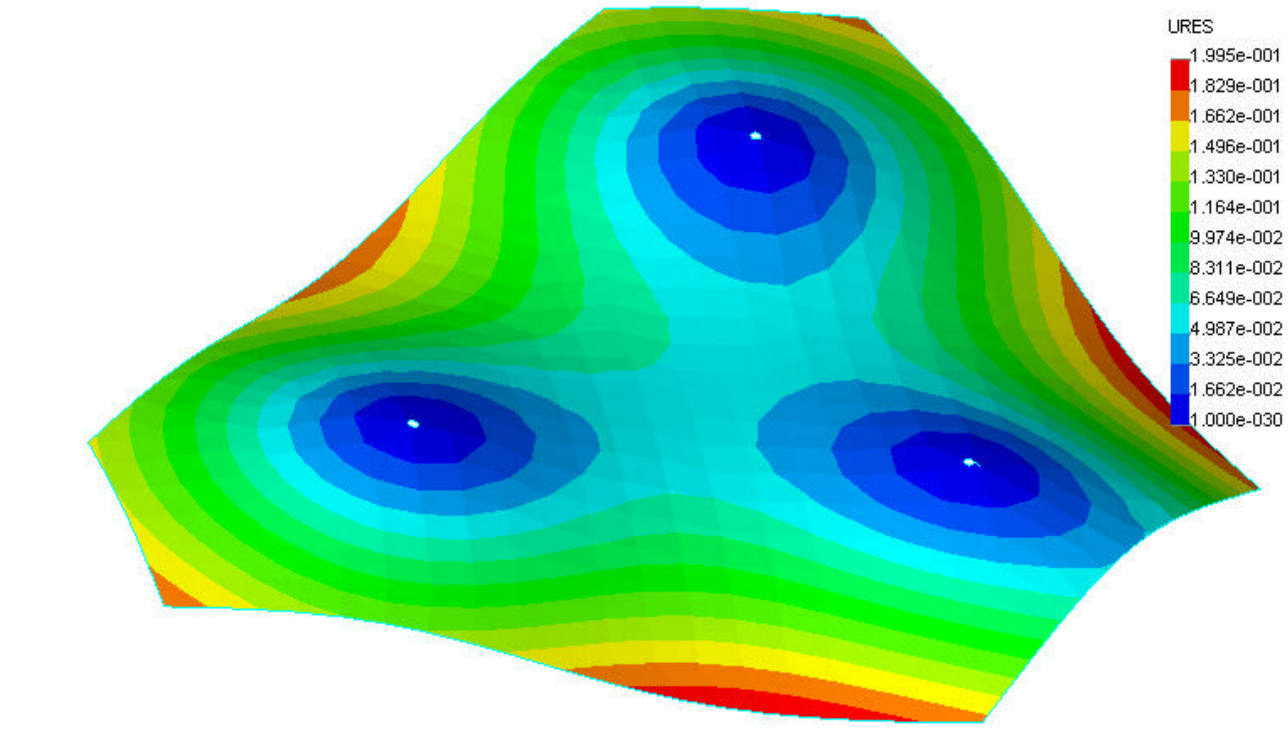

Figure 21: Simulated deflection under gravity for an individual segment supported on three fixed points before adding the active figuring system.

4.3.2. Mechanical structure

Assuring the dimensional stability of such a construction by a passive structure would be excessively massive. In order to re-use the existing building and foundations, it is therefore necessary to consider the implementation of an adaptive structure. Such structures have recently been extensively studied in the context of military applications, and its implementation in astronomical instruments is a logical step forward.

The dimensional sensors are implemented such as to measure as directly as possible the parameters acting upon the image quality of the telescope. For example, the axial position of the secondary directly relates to image defocus. The sensor to be implemented should therefore be design so as to measure this distance with a minimum of intervening mechanical structure.

The telescope can be divided into blocks consisting of one or several optical components and associated structure. This partitioning must be done in consideration of all the etapes in the life of the telescope, fabrication, assembly, test, and operation. An optical sensitivity study is the backbone of this analysis, and it should allow important simplifications in terms of assembly and test compared to classical procedures. Dimensioning elements for the adaptive structure system are:

- Measurement precision and amplitude
- Actuator resolution and amplitude
- Closed-loop control bandwidth

Control bandwidth influences upon the residual alignment errors of the optical system. For example, a 1 Hz bandwidth will handle perfectly any thermal variations (Long Term instability), but will be without action on 10 Hz perturbations (Short Term instabilities).

4.3.2.1. Structural concept

Adaptive structure consist of dimensional sensors and actuators operating in close or open loops, which allows to control in position one or several optical components (through or not structural elements).

Sensing should be able to reflect as well as possible the quality of the image, according to the parameters to control. This parameter could be, for example, the piston of the secondary mirror. The sensing will be done, for example, on an M1/M2 distance or in a better case on the concerning defocus. We will have to measure only this parameter. Disturbing elements will not have to be there; only sensing intrisic pertubating elements could be allowed. We would have to measure directly , for example, the distance between the two mirrors without including the structural elements in the sensing loop (except if their dimensional variation in the sensing direction can be neglected under the externals constraints).

Concerning the planned Korsch combination, the control could be done on different levels: - one or several optical groups
- on each individual optics

We would be able to divide the optical combination into different optical blocks. A "block" means a group of optical components and its associated structure.

The whole telescope could be cut into one or several blocks. We could considerate that the whole telescope consists on an only one block (without many interest) or that each optical components and its frame consists on separate blocks (which would be very complex to manage). The aim of the study is to consider the optimum number of blocks to keep the dimensions of the structure into the planned tolerances which allow the telescope to reach an appropriate image quality.

We have to take in account the different telescope's life step. To decide how to cut the telescope into blocks, an optical analysis is necessary. This analysis will give us positioning tolerances of each conceivable block. This cutting out should take in account the AIT (Assembling Integration Test). The assembly sequences should be simplified in comparison of a classical assembling.

We will have to determine a reference block. The definition of the blocks will take in account the different instrument life steps from the conception to the operating status.

4.3.2.2. Type of adaptive structure and associated study

Based on the three-mirror Korsch-type or four mirror optical design, a preliminary structural concept has been made (Fig. 22).

Figure 22: General view of the telescope in its eight-petal version +M4 mirror.

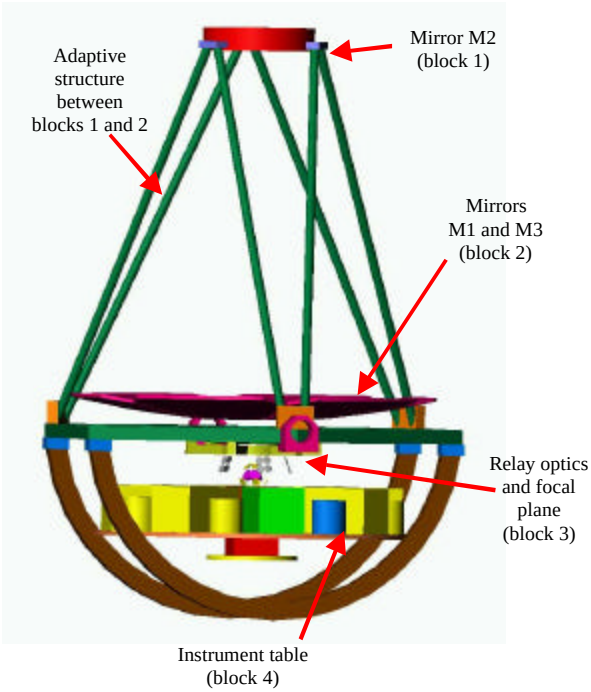

Figure 23: Tentative block allocation.

The structure is adaptive, with the following block division (Fig. 22):

- Block 1: Secondary mirror, acts as reference for the structure
- Block 2: Segmented primary and tertiary mirrors
- Block 3: Focal plane and relay optics
- Block 4: Instrument table
- Block 1bis fourth mirror

A rigorous study leading to a definite block division will be made in phase A/B, based on the following type of considerations:

- Optimal choice of reference block
- Possibility of supporting M1 and M3 in the same structural frame
- Implementation of the instrumentation, use of relay optics, etc
- Field derotation mechanism

A/ Characteristics of the adaptive structure

Between each block we will find a sensing system, an actuation system and a control loop. Thus, the different components allowing the sizing of an adaptive structure are:

- the measure accuracy
- the sensing range
- the actuation resolution
- the actuation range
- the loop frequency

Optical residual depositioning will be influenced by the loop frequency. For example, for an equal to 1 second period corrective loop , the about 10 Hz vibration range will totally operate in the residual depositioning. On the other hand, only a part of the thermic variation depositioning will be taken in account (thermic variation during the loop). The complete range of the depositioning due to the thermic variation will completely operate in the corrective range (sensing and actuation).

Then, depositioning sommations rules and associated margins must be defined. According to the proposed architectures, these data will allow to conclude to requirements about setting actuator and sensory elements.

B/ Structure's architecture: the M2 mirror maintain example

The structural study must not be derived from a past structural study, but must be viewed as a proper design philosophy, development, manufacture and implementation of an optical instrument.

We can associate a structure to the considered the Korsch optical system from the figure 13 . The optical blocks we can envisage are the followers:

- optical reference: the secondary mirror M2 (block 1)
- segmented mirror M1 et mirror M3 (block 2)
- telescope focal plan and transfer optic (block 3)

The cutting out will be discussed during the study phases A and B.This is necessary because of the following considerations:

- The position of the M2 secondary mirror is determining for the definition of the sighting axis.
- The M3 mirror is close to the M1 mirror, their distances are comparable
- There is N portions on the focal plan corresponding to N instruments and transfer optics.
- A focal plan derotation must be planned

We will envisage a global structure for the M2 mirror(block1), one for the M1 and M3 (block 2) and an other one for the transfer optic and focal plan (block3).Then, we will join blocks 1 and 2 by an adaptive structure and blocks 1 and 3 by an another one.

NB : the segmented and flexible mirrors fact is not taken in account on the adaptive structure level but as an independent active optic. It means that the loop frequency will be different from the adaptive structure's one. We will keep it in mind for the interface level.

A possible architecture is proposed on figures n° 22.

To determine the characteristics elements requirements of the viewed adaptive structure, we will study its performances concerning depositioning under environmental and operational constraints.

It means that we have to evaluate each contributors from the under board grey parts.

Overall performances			
Telescope optical performances		**Detector and instrument performances**	
Optical theoretical performances	**Optics manufacture performances**	**Optics depositioning performances**	
		Decentering	**Piston**
Diffraction (bias)	Polishing (bias)	Integration (bias)	Integration (bias)
Residual Aberrations (bias)	Residual gravity effects on the optics (LT)	Thermo (ST + LT) and hygro-elastic (LT) stability (according the material)	Thermo-elastic stability (ST + LT)
...	Mirror integration/ frames (bias)	Mirrors supports (LT)	Hygro-elastic stability (LT) (according the material)
	...	Wedging bias (bias)	Gravity (LT)
		Gravity (LT)	Transfer optic (bias + LT)
		Ageing (LT)	…
		µ-vibrations (ST)	
		...	

ST: Short Term - LT: Long Term

The study of each post for a determined architecture will allow to evaluate the correcting necessary range and according to the searched performances will allow to determine the loop frequencies, the actuators resolution and the sensing accuracy.

NB: An important point in the definition of the adaptive structure is its interface in terms of mechanisms and control frequencies with the active control of the primary mirror.

The figure 22 structure is strongly adapted to a secondary mirror positioning. Thus, there is a bijective application between the six rood elongations and the six mirror degrees of freedom.

In other words, to each configuration representing an elongation state of the six rods corresponds one and only one position of the mirror M2 (for small movements). Conversely, for each position of the mirror M2 corresponds an elongation state of the rods.

Thus sensing (if it consists of linear sensors) between the mirrors M2 and M1 will have the same geometry as the rods. Moreover this geometry have the advantage to distribute the sensitivities in the good directions: greatest sensitivity in defocus and tilt and less sensitivity in decenter (weak for the tilt around the optical axis). It is significant to note that one takes measurement directly on the mirrors and not along the rods.

4.3.2.3. The mounting

The optical systems considered have their focal plane in the prolongation of the telescope optical axis. The instruments move in rotation with this focal plane.

Various equatorial mountings seem unsuited here because of the significant suspended masses. Such mounting would involve an overhang with intolerable encumbrance.

Mounting suggested here (fig 24) includes two standard " horseshoe " and two traditional stages with bearings (standard and size of those of the VLT (TBC)). The two standard "horseshoes" limits the efforts on the traditional stages. They are hydrostatics oil pads type and supports the majority of the loads due to gravity. The two traditional stages guide the whole around the telescope horizontal axis. The efforts induced on these stages are residual loads: the size is then close to those of the VLT (less development to be considered). The vertical axis is like those of large radio telescope (hydrostatics oil pads type).

The overall diameter on the ground does not exceed the actual size building. In the same way, if we use carbon/epoxy frames and trusses the mass of such structure should not be much more significant than that of the current telescope + mounting (for one 16 m diameter). By considering a reduced cupola, one could consider a mass of the same order for the whole telescope.

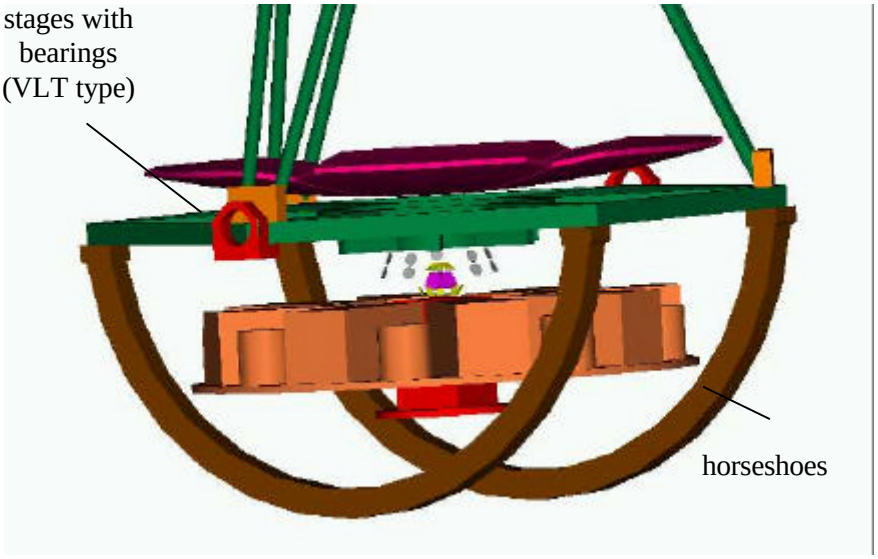

Figure 24 : horizontal axis of the mounting

4.3.2.4. instrumentation supporting plate

One benefits from the big size of the primary mirror to put below this one a platform accommodating the various instruments. Those can be 4 in the centre from the field and 6 to 8 (TBD) on the periphery. The derotation of the field is carried out on the transfer optics level and on the platform level which supports the instruments. Moreover these two functions make it possible to consider the redistribution of the transfer optics to the various instruments and the change of the instruments by a rotation of the platform.

A/ The transfer optics

There principal functions are:

- to select part of the field in the focal plan of the telescope
- to transport the image until the entrance of the instrument
- to stabilize the image with the entrance of the instrument

- to possibly create an intermediate pupil to carry out a tip-tilt wave front correction or other.

There are various solutions making it possible

- " optical fibre bundels " of the Giraffe type

The fibres can be distributed:
- individually as light collector without transmission of space information
- in small groups (IFU) distributed on more or less wide objects (preserved space information)
- grouped in a more significant given spatial field (Argus mode)

The derotation is followed by optical fibres undergoing an acceptable torsion. Any instrument displacement compared to the telescope focal plan is compensated by fibers attached on the focal plan and the instrument

- .an optical mirror relay with access to the pupil (fig 25)

In such a relay in addition to the field lenses we have a collimating and a camera unit with mirrors, We have also a tip-tilt and/or deformable mirror in the pupil.

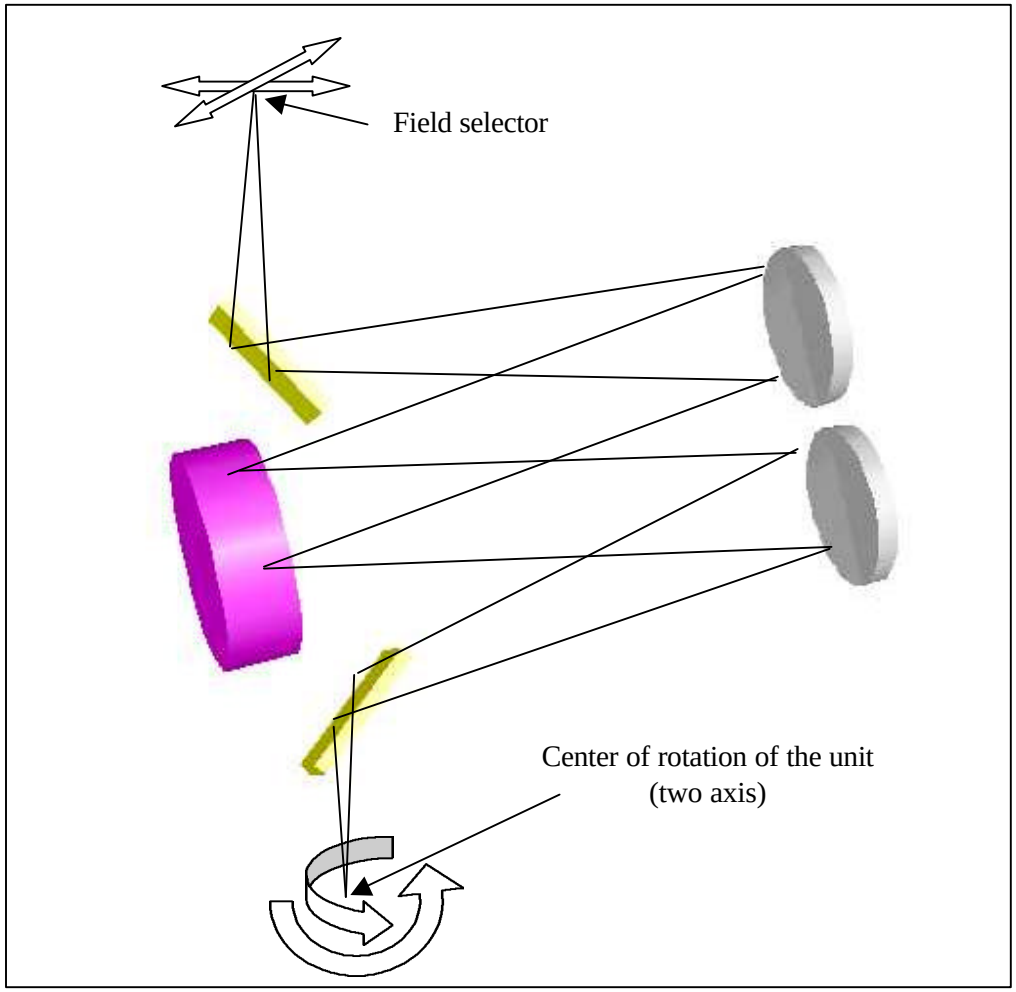

Figure 25 mirror relay with access to the pupil

Such a system allows a puncture of the field in a broad zone.

B / the instrumentation supporting plate

This plate is supported by the arches of the " horseshoe ". The overall rotation should not be of high degree of accuracy since that accuracy is deferred to the level of the field selection This unit is in rotation to compensate for the great movements. However fluid stages would be appreciated on this level to compensate the significant masses and to avoid vibrations.

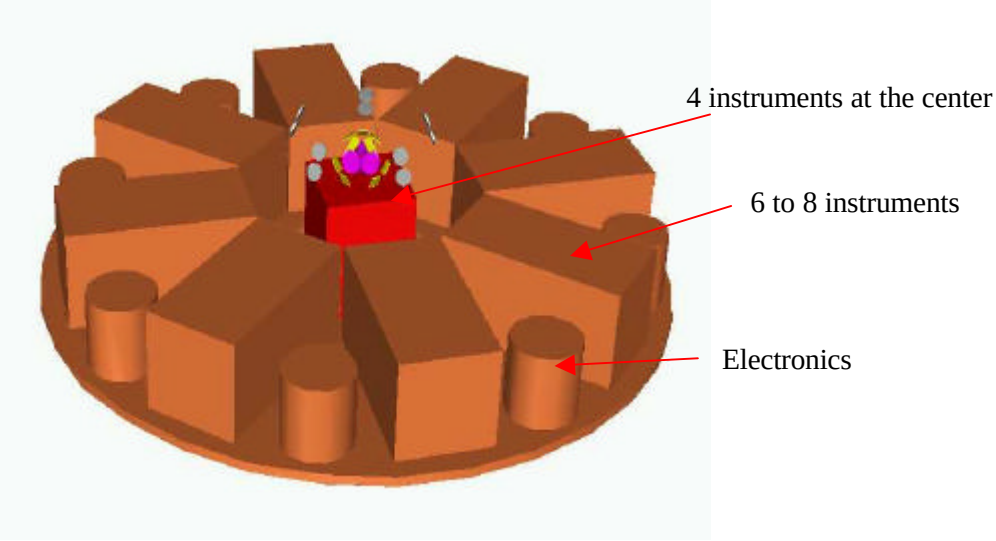

Figure 26 instrumentation supporting plate

4.3.3. Dome/building

The preliminary concept is based on a VLT-type dome mounted on the existing pillar (Fig. 27). During phase 2 we will investigate more thoroughly the dome/pillar/foundation configuration concept with respect to mass, thermal effects, air flow and wind loading. General infrastructure questions should also be considered, including coating plant, and other auxiliary activities.

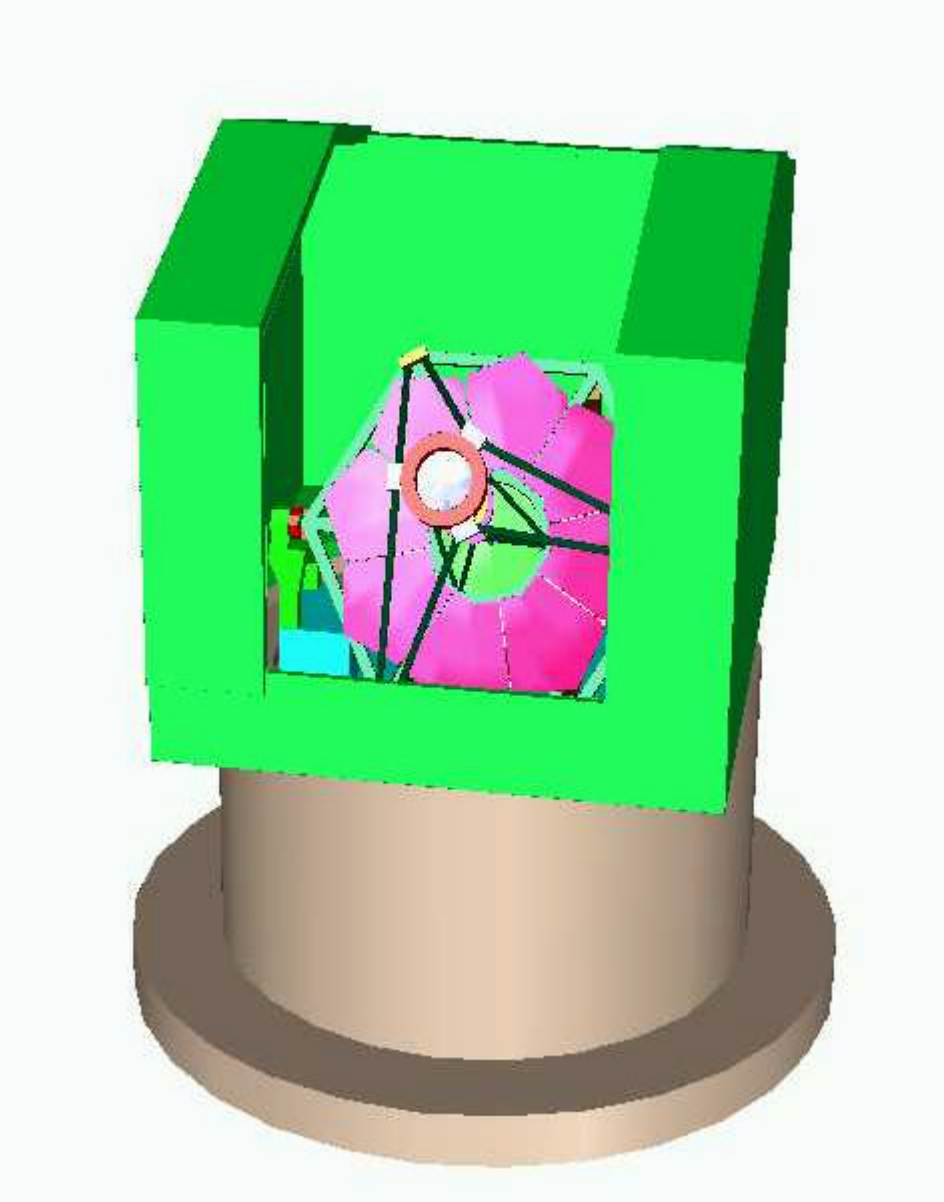

Figure 27. Conceptual dome design conserving the existing pillar.

4.4. Key technologies

4.4.1. Mirror manufacturing

The realization of the currents 8 and 10-m telescopes has been possible with only substantial developments and industrial efforts made during the last decade, including the two major fundamental concepts: segmentation and active optics. In theory, segmentation allows any size extrapolation without scaling fabrication processes and active optic relaxes fabrication tolerances and allows automated control of optical quality.

These two technologies not only drive telescope optical design but also optics fabrication, and the planned next generation telescopes, as the concept proposed for CFHT replacement, thoroughly include both concepts.

As demonstrated within the VLT project, active optics systems allow increasing and maintaining mirror performance in real time. Active optics, due to the relaxation of surface tolerances and the possible use of less classical material, has also advantage in cost reduction and feasibility. The induced drawbacks, like the added system complexity (at operational and maintenance levels) and the sensibility to frequencies higher than the control-loop, are well identified and controlled in the present generation of large telescopes.

The main advantages of segmentation are scalability and cost reduction. This latter is even more efficient in the case of identical segments, for spherical primary mirrors or with a limited number of large aspheric ones.

With passive segments in the 1- to 2-m range, the solution using a spherical primary mirror is certainly the most effective as it allows for segments mass-production. However, as the segments are passive, a tight tolerance has to be imposed on the curvature of the different segments, leading to a severe material selection (homogeneity of thermo-mechanical properties). For the 8-m class segments considered in the NG-CFHT proposal, this tight tolerance can be reduced, as the surface figure will be actively controlled, and thus leading to a cost reduction.

The realization and testing of off-axis aspheric surfaces is obviously more difficult than generation of spherical ones, however this problem has already been solved during the last decade, by using computer-controlled polishing and testing. The manufacturing of a limited number of large and identical off-axis aspheric segments does not seem to be critical point. With a limited number of segments the problem of surface discontinuities is also reduced and the phasing by using position sensors is less complex. This drawback (discontinuities and phasing) may completely disappear with the development of new piston sensor techniques.

In the NG-CFHT proposal three optical configurations are considered: a Ritchey-Chretien (RC), a four mirrors (4M) and a three mirrors (3M) designs. A preliminary trade-off between the proposed solutions, relatively to the mirror manufacturing difficulties, is mandatory. This phase has been realized in close collaboration with an optics manufacturer (REOSC-SAGEM) and a copy of his report and conclusion can be found in Annex.

4.4.1.1. Mirror M1

In the proposed designs, the 20 m primary mirror is constituted of 8 off-axis aspheric 8-m class mirrors (Fig. 20). If spherical segments are certainly easier to manufacture such design have limited FOV and require a highly aspheric corrector whose testing is still difficult. According to the optics manufacturer REOSC-SAGEM, the cost difference between off-axis aspheric segments and spherical segments is likely to be negligible once the realization and test of the highly aspheric corrector are included.

The irregular hexagon or octagon form of the segments implies careful attention to be paid to stress and strain releases during the cutting process.

4.4.1.2. Mirror M2

The major difference between the various designs is the secondary mirror size. In the RC and the 3M configurations this mirror has a 6-m diameter while is only 3-m in the 4M solution.

The manufacturing and testing of a 5-m convex aspheric mirror is certainly the most complex point. Testing the complete surface in one shot is not feasible and a surface reconstruction technique, from partial interferograms will be necessary. Taking into account a 1-m secondary central obscuration, a 2-m reference gauge can be used to control the mirror on its radius and the final surface figure reconstructed from multiple tests with overlaps. The 2-m reference is a critical point as a good material homogeneity in such a large piece of refractive optic is difficult to obtain. Lens with a reduced diameter (1.3-m) would be easier to manufacture but the testing will then require using two different null-lenses for the inner and outer parts of the mirror. This will lead to a larger number of sub-tests and a more complex algorithm to reconstruct the entire secondary surface. The use of a computer-generated hologram could be a solution to test this large convex asphere. This possible test set-up has still to be investigated and if no practical solution is found, a design with a smaller secondary mirror will have to be considered.

The 2.5-m mirror in the 4M configuration is a more classic optic and its realization does not generate any particular problem. The manufacturing could be done by ion-beam figuring for a size slightly lower than 2.5-m as this is the actual limit size of the mirror manufacturer ion-beam tools.

4.4.1.3. Mirror M3

This mirror, in the 3M and 4M configuration, is a 6-7 m concave aspheric surface with no particular difficulty.

4.4.1.4. Mirror M4

In the 4M design, this mirror is flat with a 3.3-m diameter. As for the M2, the use of a reference gauge is necessary to test this mirror, but its flat shape reduces the problem somewhat. A slight design change permitting the use of a concave mirror with a sufficiently short radius of curvature to allow centre-of curvature testing (~40 m) would be a great advantage from a manufacturing point of view.

4.4.1.5. Conclusion

The realization of the different mirrors, for the various optical designs considered, does not raise any fundamental impossibility. Some modification of the designs could facilitate the manufacturing of mirrors and a complete trade-off, in terms of cost and production time, has to be performed. The mirror manufacturer (REOSC-SAGEM) is confident that if a test set-up is possible, any surface can be generated.

4.4.2. Adaptive structure systems

The novelty of the adaptive structure concept proposed is its integration within the telescope structure. Developments of metrology systems will be required within the fields of mirror positioning, primary phasing, and segment shaping. This follows naturally from the R&D activities carried out in our laboratories. Mechanical actuation concepts will also require further studies: low-resolution, large-range actuation systems, and high-resolution, medium-range actuation systems. Technological evaluation and validation will require construction of functional demonstrators. In phase two we will make a technological roadmap for the required developments.

4.4.2.1. Sensing unit

The system of measurement must be an absolute sensing unit. It must allow sensing of several tens of meters with micrometer resolutions. It should not disturb the environment (parasitic lights, variation in temperature, an so on).
The major requirements is to constitute an absolute zero at a distance of several ten meters, adjustable but stable up to few micrometers in time or well easily adjustable. Around this absolute zero, one wishes to lay out a relative system of measurement for some hundred millimeters with a resolution of some micrometers.
There are many interferometric systems of measurement answering in the majority of constraints mentioned above. However, few ones present a system of absolute sensing

A/ Aerial system in white light

The transducers are divided into six sensing beams of measurement (figure 28). We still need reference beam. One can plans to use the dimensional stability of the primary mirror in Zérodur to create a reference having an adapted dimensional stability. The system uses the integrated optics and a piezoelectric actuator to adjust the absolute zero (system developed by the laboratory of Photonic Systems in Strasbourg)

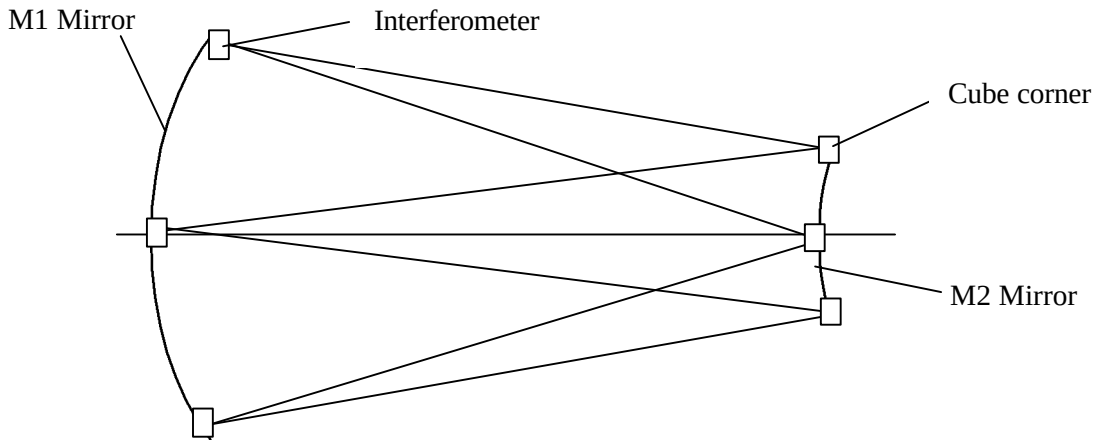

Figure 28 transducers configuration

The principal assets of such a system are:

- the feasibility of the interferometer
- the completely static measurement of phase;

The principal disadvantage is:

- the use of the system is sligthly sensitive to the air temperature

B/ Aerial System using several wavelengths

The configuration of the sensing units is the same one as for the A system. A measurement with an interferometer with only one wavelength becomes ambiguous when the difference of optical path exceeds the wavelength value. The use in an interferometer of two wavelengths $\lambda 1$ and $\lambda 2$,, makes it possible to be free from intrinsic ambiguity to any measurement of phase on a more significant range. Indeed, the difference between the phase measurements obtained with these two wavelengths makes it possible to generate a differential phase E which removes the previous ambiguity so far as the resulting wavelength Λ is large compared to the double of the sensing range (2λ). One gets:

$$dL = E \times \Lambda \text{ with: } \quad \Lambda = \frac{l_1 l_2}{l_2 - l_1} \quad \text{and: } \quad 0 < E < 1$$

One can consider a Michelson interferometer into which one will inject two wavelengths that one will separate at the exit in order to send them on two detectors.

This device allows, by choosing sufficiently distant wavelengths ($\Delta\lambda$=200 nm), to take very precise measurements (about 0,1 µm), but on a narrow range (lower than 2 µm). To increase the measurement range, it is necessary to bring closer the wavelengths (with a less precision). One can thus consider an interferometer with three colors: two very close and one distant. One thus takes the first measurement using the two close wavelengths to fix the range of value, then one takes a second measurement using the two more distant wavelengths to get the precise value. Precision for the first measurement have to be lower than the range of the second measurement. The measurement of the phase can be carried out using a modulator placed on the reference beam which makes it possible to visualize on the detector a phase shift compared to the nearest maximum.

This device has the following advantages:

- the system is compact since there are interferometers using integrated optics;

The device presents the following disadvantages:

- the sources must present significant lengths of coherence (higher than the double of the length to be measured);
- the system of phase detection is active.

The sources could be lasers diode stabilized in frequency with which one associates an interferential filter. It will be necessary to demonstrate the feasibility of such sources.

C/ System of measurement by EOH

This technique allows the measurement of the distance variations between a mirror and a sensor fixed on another optical element. One measures displacements of small images created by EOH (Optical Elements Holographic) stuck or engraved on a mirror. This principle has been tested on a ground based telescope from Lockheed Missiles and Space Co.

The principle is the following:

The telescope (Cassegrain system for example) works in a completely traditional way (see the figure above): the signal of the object to be observed falls on the M1 mirror, is reflected on M2 before reaching

the focal plane. Simultaneously, a camera is illuminated with the same aperture ratio as the one of the telescope using a source (a laser for example). The beam will be stopped down by a hole located in the focal plane of the telescope. It thus plays the role of source. The light is reflected then on a mirror which could be a dichroic blade, as an example, in order to allow a maximum transmission of the light towards the focal plane of the telescope. After that the light of the source will traverse the telescope in the opposite direction and thus will be collimated by the telescope. On the primary mirror, one sticks or one engraves small circular holographic gratings which will diffract the light of the source. The zero order which constitutes more than 95% of the light will put the image of the point source to the infinity. The first order will be directed towards the center of the secondary mirror, on a sensor located close to the focal plane of the M1 mirror. We thus will find again on the sensor the images of the source limited by the hole (see the figure below).

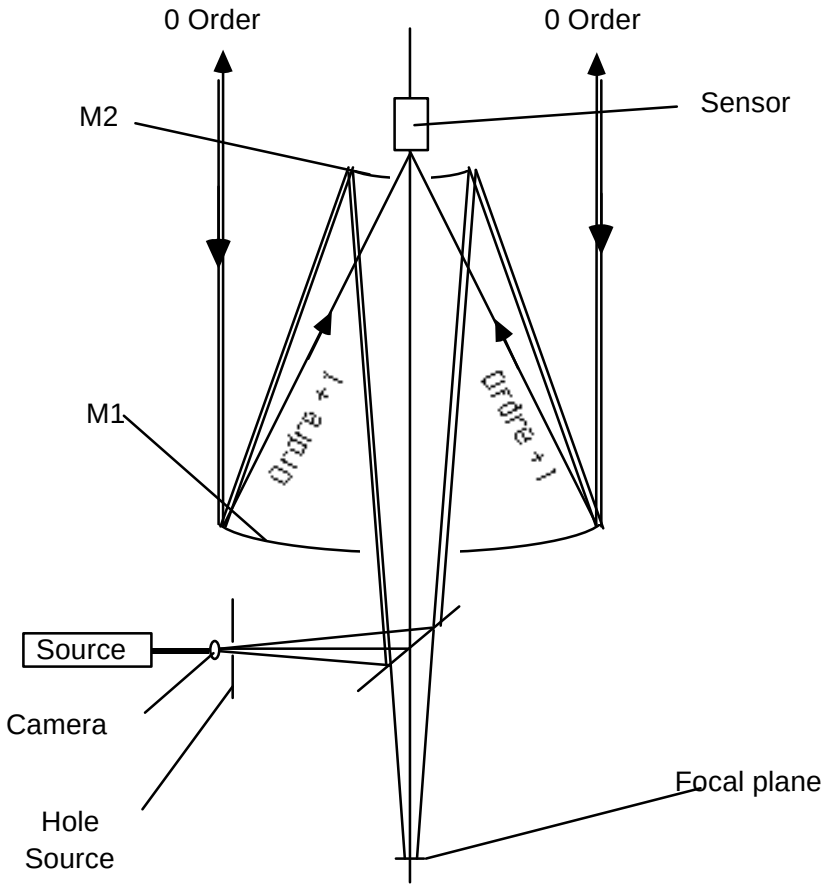

Figure 29 System of measurement by EOH

The position of the diffracted images on the sensor makes it possible to evaluate defocusing, decenterings, tilts as well as the aberrations of the 3rd order In practice, one will create a plane wave at the exit of the source which will be diffracted by the holographic grating. That simplifies the recording of the grating which will be done by using a plane reference wave front if dichromate gelatine is used (photosensitive resin). One can plan to engrave this grating by microlithography... Such a system does not depend any more an the observed object. One can thus carry out control apart from a phase of observation, which releases the information processing system from longtime calculations. One can however consider some corrections during the acquisition of the signal since the output of the holographic grating is very bad (particularly far away from the working wavelength). With thin system one will have a few percent of the light around the working wavelength diffracted in the first order and nothing in the higher orders: almost all

of the light will be in the zero order. Thus the disturbance on the pupil is tiny but will have to be evaluated precisely. The precision and measurement ranges will put constraints for the sensor characteristics. The sensor performances will depend in particular of:

- the uniformity of the deposit of the resin;
- the sensitivity of the resin;
- the optical quality of the recorded waves;
- the developer and fixing solution used for the grating after recording;
- the maintenance of the mirror.

The technological studies which would be necessary for such a system thus concern:

- the technique of recording;
- the optical quality of the recorded waves;
- the realization and setting up of the distributed gratings on the primary mirror.

This system is well adapted to the positioning of the secondary mirror compared to the primary one. Its use for other optical elements seems also possible.

4.4.2.2. actuator units

The actuators will be structural ie they will have to transmit the efforts. However in the case of the structure of figure N, the rods have knuckles on the level of the actuators. One will be able to thus propose actuators provided with elastic pivots (with a possible central axis). The actuator works then primarily in traction/compression.

A/ The mechanical actuators

They are of rollers screw type, with blades and mechanical amplification. These actuators have to be developed according to the constraints defined by the structure.

B/ The hydraulic actuators

They are of the double-acting jack type and will have to be calculated according to the constraints defined by the structure. However, an example is proposed on the figure below.

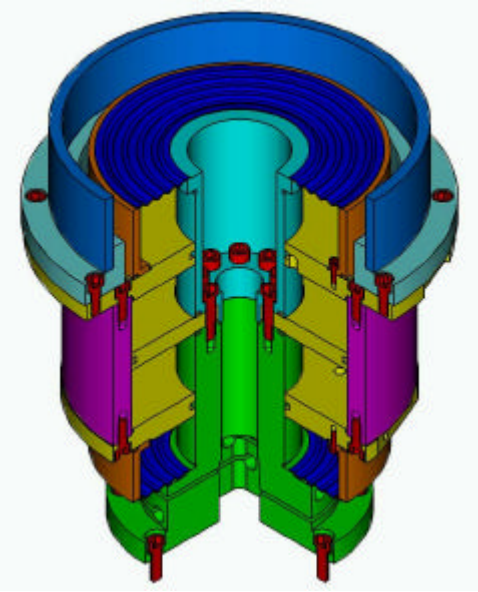

Figure 30 The hydraulic actuators

4.4.3. Adaptive optics systems

In order to obtain images with diffraction limited spatial resolution, Adaptive Optics (AO) systems must be implemented to correct atmospheric perturbations. For our telescope proposal, we consider three different AO concepts:

- Classical AO, diffraction limited over a field of view of a few arcsec.
- Multi-Conjugate Adaptive Optics (MCAO) using multiple deformable mirror and complex wavefront sensors to recover tomographically the atmospheric turbulence over a 1' field of view.
- Low-order AO to provide angular resolution of about 0.2" over a field of view of up to 3' using tomographic wavefront sensing.

Although low-order perturbation correction can be achieved with conventional technology (for example, stacked piezoelectric actuators with thin flexible mirrors), high order correction for a 20m telescope would requires a prohibitive number of actuators for this technology. Development of new devices based on MOEMS (Sec. 4.4.5) is therefore of great interest for our project. Due to their compactness and replicability, these micro-optical components are also perfect candidates for numerous low-order AO buttons.

4.4.4. Micro-optics

MOEMS are designed for a wide range of applications like sensors, switches, micro-shutters, beam deflectors, and micro-deformable mirrors. The main advantages of micro-optical components are their compactness, scalability, and specific task customization using elementary building blocks. As these systems are easily replicable, the price of the components is decreasing dramatically when their number is increasing. They will be widely integrated in next-generation astronomical instruments, especially for space missions, as they allow remote control. The two major applications of MOEMS in astronomy are Multi-Object Spectroscopy (MOS) masks and deformable mirrors for Adaptive Optics (AO) systems.

4.4.4.1. Principle

MOEMS technology is closely linked to the micro-electronics fabrication process. Various materials are deposited on the surface of a substrate, and, using masks, their localization on the substrate is precisely defined in order to ensure their specific tasks. In micro-systems, there are two kinds of layers: structural layers and sacrificial layers. The structural layer materials are polysilicon or metal, and the sacrificial layers are silicon oxides or organic materials. The sacrificial layers are chemically dissolved at the end of the fabrication process in order to create air gaps between the remaining structural layers. A great level of sophistication in the micro-electronics technology ensures excellent tolerances on layer thickness and patterning precision.

Micro-mechanical actuation is obtained using electrostatic, magnetic or thermal effects, but the most advanced actuation is achieved by the electrostatic effect. The electrostatic actuator consists of two electrodes of metal or polysilicon heavily doped with phosphorous, isolated from each other by a gap of thickness g filled with dielectric medium, usually air.

When a voltage V is applied between the electrodes, an attractive force F is generated, and if one of the electrodes is mobile, it moves toward the other. By neglecting edge effects and bending of the electrodes, i. e. assuming good stiffness of the electrodes, the instantaneous, nonlinear electrostatic force F is defined by the following relationship of key parameters:

$$F = \frac{AeV^2}{2g^2}$$

where A is the overlapping electrode area and e is the dielectric constant in the inter-electrode spacing. Assuming h the initial inter-electrode gap (without voltage), and x the deflection of the upper electrode, the value of g is decreasing from h to $(h - x)$ when the upper electrode is moving. The accessible motion is generally limited to $x < h/3$. At this limit, the nonlinear electrostatic force increases more rapidly than a linear restoring force, applied for example by springs attached to the upper electrode. The electrostatic effect then becomes unstable and the mobile electrode drops toward the fixed electrode and sticks to it.

In the design of MOEMS components, various parameters have to be tuned. These parameters differ according to the functionality of the component. We will consider two different devices, a Micro-Mirror Array (MMA) for MOS and a Micro-Deformable Mirror (MDM) for AO systems.

An MMA is an array of electrostatically driven bistable mirrors, with a size of a few tens of micrometers, which can occupy two discrete positions, ON and OFF, with switching times of a few microseconds. The two positions are obtained when the mirror hits physically the substrate, using the electrostatically induced motion until its unstable portion. Specific parameters for this device are the tilt angle and the actuation voltage. The tilt angle determines the separation between the input beam and the output beam and therefore the possible numerical aperture of the instrument. A large tilt angle also reduces the scattered light of the array entering the output pupil. However, the fabrication process is not compatible with the use of very thick sacrificial layers on top of the substrate, limiting the tilt angle. The two discrete positions are typically rotated ±10° with regard to the substrate plane, producing a 40° beam separation. The second parameter is the actuation voltage: its value has to be low enough for matching the performances of integrated driving electronics.

MDM are constituted by a reflective surface with an underlying set of actuators driven in the linear portion of the electrostatically induced motion. For MDM, key aspects are inter-actuator spacing, inter-actuator coupling, actuator bandwidth and low driving voltage. High order wave front correction needs a large number of actuators. The size of conventional Si wafers limits the maximal size of single deformable mirrors, increasing the required density of actuators. Typical inter-actuator spacing could be in the range 200-500 µm. An inter-actuator coupling factor can be defined as the ratio of the motion of an actuator with no voltage applied to the motion of a neighboring actuator in action. If this factor is close to 1, there is too much redundancy, the effective actuator number is drastically reduced and high-order deformations cannot be corrected properly. If this factor is zero, sharp slopes are present on the surface, usually on top of the actuator location, resulting in larger residual wave front errors. If this factor is 20-30 %, the surface has a smooth overall shape with low residual errors.

For both MMA and MDM devices, three additional parameters are of interest: the optical surface quality, the driving electronics and the actuator bandwidth. As these micro-optical components include mirrors, their surface quality must be excellent. We have developed an original method based on Foucault's knife-edge test for the surface characterization of individual MMA micro-mirrors. The driving electronics is also a challenge as the high number of actuators integrated on a semiconductor substrate leaves individual actuator driving impossible. The driving circuit has to be integrated on the wafer or directly bonded to the optically active elements. The driving voltage must then be as low as possible, a few tens of volts is preferable to the several hundreds of volts often used in present-technology devices. The design of driving circuits requires much attention in order to match the needed bandwidth, and to be compatible with the technology employed to realize the mobile mirrors on top of the electronic driving circuit. Finally, the bandwidth of these components must match the specific requirements.

4.4.4.2. Micro-Mirror Array for Multi-Object Spectroscopy

In order to obtain spectra of hundreds of objects simultaneously, MOS require a reconfigurable multi-slit device. Conventional masks are made by laser cutting or by using complex fiber-optics-based mechanisms. A promising solution is the use of an MMA for generating reflecting slits (Burg 1998, Burgarella 1998). By placing the MMA in the focal plane of the telescope, the light from selected objects is directed towards the spectrograph, while the light from others objects and from the sky background is blocked in a light trap (Fig. 31). MMA allows remote control of the multi-slit configuration in real time.

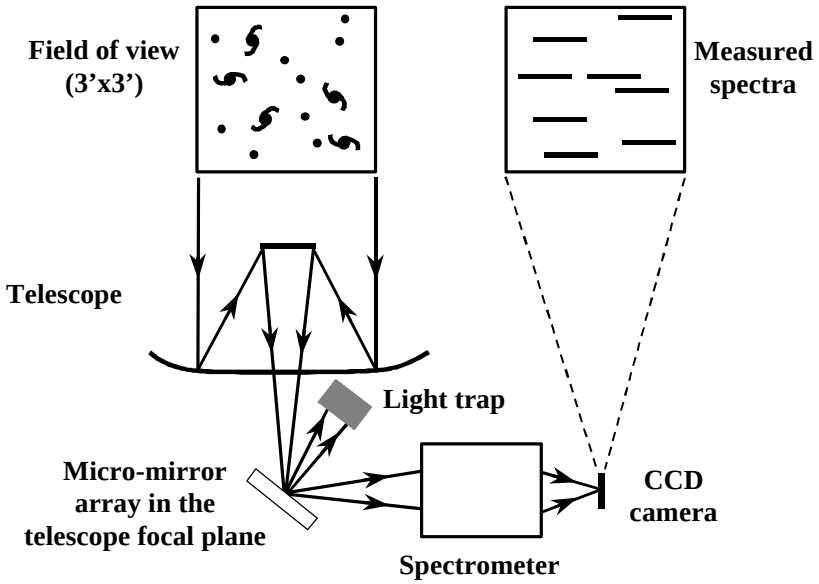

Figure. 31: Principle of Multi-Object Spectrograph with a Multi-Mirror Array.

We have based our work on a most impressive MOEMS realization, the MMA designed by Texas Instrument for video projection, which is an array of 1K x 1K, 17 µm pitch bistable mirrors (Hornbeck 1995). A picture of the micro-mirrors is shown in Fig. 32. These electrostatically driven mirrors can occupy two discrete positions (ON and OFF), rotated ±10° with regard to the substrate plane. The switching time is a few microseconds. Using this MMA, any required slit configuration might be obtained with the capability to match point sources or extended objects (Fig. 21). In the park position, i.e., without driving voltage applied, the micro-mirrors are undeflected, parallel with the substrate. In action, the micro-mirrors in the ON position direct the light toward the spectrograph and appear bright, while the micro-mirrors in the OFF position are dark.

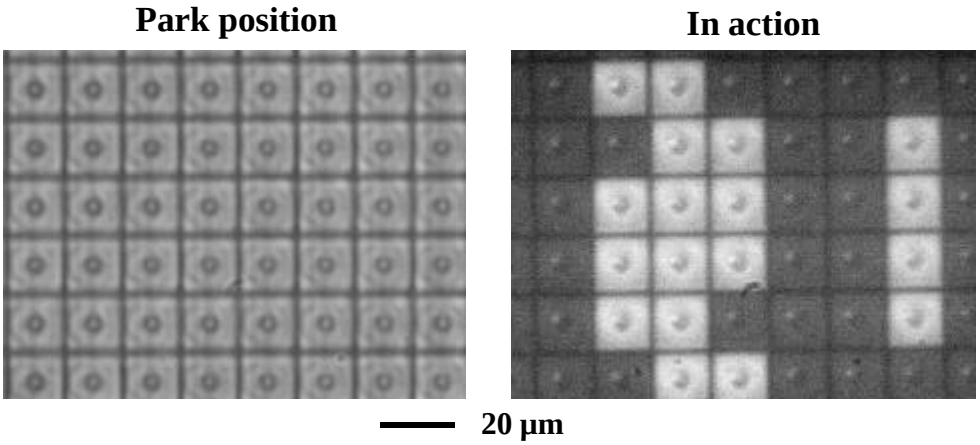

Figure. 32: MMA in park position and in action with various "slit" shapes.

The Laboratoire d'Astrophysique de Marseille (LAM) is the only European laboratory to have participated in the NASA study of a near infra-red MOS equipped with tiltable micro-mirror array (MMA) for NGST (NGST-MOS study, PI John MacKenty). With the aim of including this micro-optical device in a MOS, we have directed our studies along three lines:

- Surface characterization of individual MMA micro-mirrors by an original method based on Foucault's knife-edge test.
- MMA optical modeling by ray tracing.
- Optical design for the MOS including two different concepts.

For testing micro-optical components, development of accurate surface characterization methods is essential. The most commonly used techniques for surface characterization are based on interferometry, but on a micron-sized regular array with deep discontinuities the results obtained are dramatically affected by diffraction effects. To overcome these effects, we have introduced a novel surface characterization method with an incoherent light source (Zamkotsian 1999-1, 1999-3), based upon Foucault's knife-edge test (Foucault 1859). We have used this technique to characterize the MMA designed by Texas Instruments (Hornbeck 1995). Our measurement indicates a maximum slope below 1 mrad and surface deformations smaller than 2 nm. Each micro-mirror has a "palm-tree" shape, which can be explained by strain relaxation in the thin aluminum layer constituting the mirror surface. A slope map for 8x6 micro-mirrors reveals slight mirror-to-mirror shape variations, notably due to combinations of tilt and astigmatism (Zamkotsian 1999-3).

Optical design of the multi-object spectrograph requires a ray-tracing equivalent of the MMA. Using the non-sequential ray tracing ability of the Synopsys program, we have simulated a block of nine micro-mirrors with individual tilt angles, and, by locating blocks of micro-mirrors in critical field locations, we are able to properly design an MMA-MOS. We have studied different concepts for the MOS: a spectrograph with focal reduction, and a unit-magnification spectrograph preceded by a focal adaptator (Zamkotsian 1999-2, 2000-2).

4.4.4.3. Micro-Deformable Mirror for Adaptive Optics Systems

The second major application of MOEMS in future instrumentation is in the field of deformable mirrors. LAM is involved since June 2000 in the European Research Network on the conception of Adaptive Optics systems for Extremely Large Telescopes. The micro-deformable mirrors (MDM) of these systems should be able to reach a large number of actuators (> 100 000) and small inter-actuator spacing (few 100 µm). Due to limitations in conventional technologies, we have based our new deformable mirror concepts on MOEMS technology. We are currently engaged in the definition of required technologies, materials and tests structures. These compact, lightweight and low-consumption deformable mirrors with on-chip electronics will enable the correction of wave front perturbation in highly integrated astronomical instruments (Fig. 33).

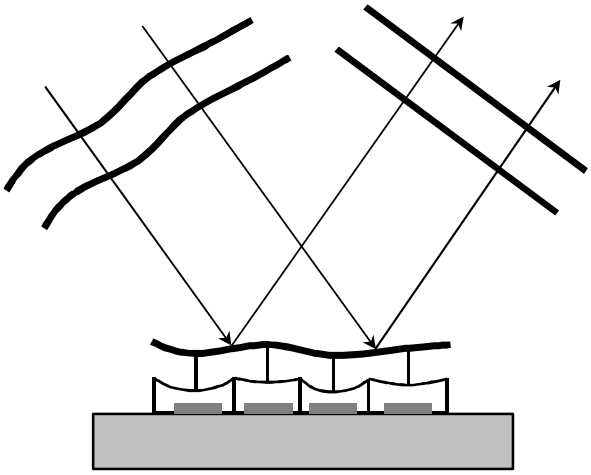

Figure 33:
Principle of wave front correction using a Micro-Deformable Mirror (MDM).

Three main MDM architectures are under study in different laboratories. First, the bulk micro-machined continuous-membrane deformable mirror, studied by Vdovin from Delft University, is a combination of bulk silicon micromachining with standard electronics technology (Vdovin 1997). This mirror is formed by a thin flexible conducting membrane, coated with a reflective material, and stretched over an electrostatic electrode structure (Fig. 34 (a)). Local deflections of the membrane are obtained by applying different voltages to the electrodes. This deformable mirror has a continuous flexible mirror with a very good surface quality and a large deflection, but for a low inter-actuator coupling, inter-actuator spacing $l < 1$ mm cannot be reached, reducing therefore the number of possible correction modes. The thin and large suspended flexible mirror is also rather fragile and removing fabrication stresses is very difficult. Finally, increasing the surface of the suspended membrane is not obvious.

Second, the segmented, micro-electro-mechanical deformable mirror realized by Roggeman (1997) at University of Michigan and Cowan (1998) at Ohio Air Force Research Laboratory consists of a set of segmented piston-only moving surfaces, fabricated in dense array (Fig. 34 (b)). The piston-like motion is obtained by applying a voltage between the active mirror area and an underlying address electrode. Due to the large static background, the segmented deformable mirror has a low optical efficiency (typically 40%) and large interference effects. The driving voltage is remarkably low (15 V), but the actuation efficiency (stroke/driving voltage) is comparable with the previous architecture. This device offers the highest degree of freedom and simplest control algorithms because each segment is completely independent. The segment density can be adapted to the needed aberration correction (low order, high order) and the piston motion can be increased with a larger gap between the electrodes.

Third, the surface micro-machined continuous-membrane deformable mirror made by Bifano (1997) at Boston University is based on a single compliant optical membrane supported by multiple attachments to an underlying array of surface-normal electrostatic actuators (Fig. 34 (c)). This type of deformable mirror allows a continuous control of the membrane's local deformation with nanometer precision at the attachment points, and a frequency response exceeding 50 kHz. The number of actuators is not limited and they can be driven with an underlying electronics in the silicon substrate. High optical efficiency and minimal diffraction effects can be achieved. Main disadvantages of this architecture are small-scale print-through deformations on the optical surface due to the fabrication process, weak inter-actuator coupling and rather high driving voltage. The resulting actuation efficiency is lower than the values obtained with the two previous architectures, mainly due to the stiffness of the structure. Another critical issue is the realization of a mirror layer without any stress, since the deposition of a thin layer on a large surface cannot be achieved without residual stress. The solution adopted by Perreault (1999) is a segmented tip-tilt mirror with anchoring posts shared between four square adjacent segments in order to ensure the optical phase continuity of the mirror. Unfortunately, this solution leads to diffraction effects already discussed in the second type of MDM. This is certainly the most promising architecture, but low actuation efficiency and mirror surface quality need further improvement.

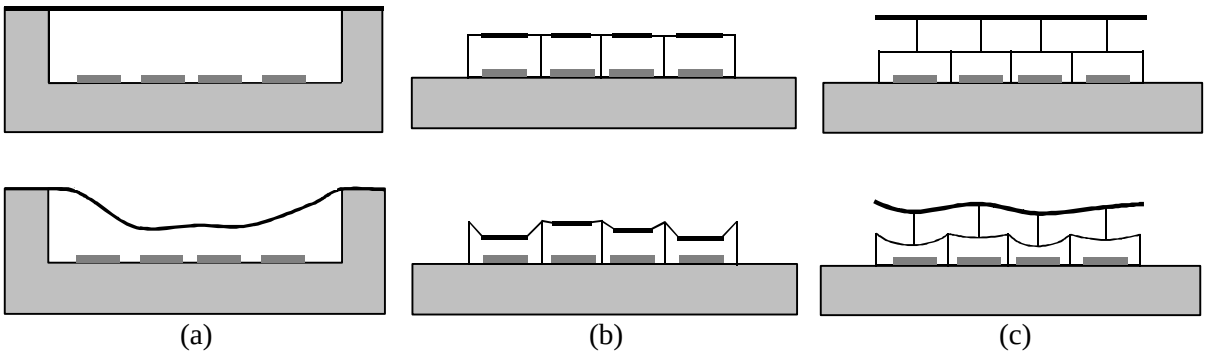

Figure. 34: Three different architectures of MDM, in the rest position (upper panels) and in action (lower panels).

These three architectures, bulk micro-machined MDM, surface micro-machined continuous membrane MDM and segmented MDM, are the three main electrostatic MDM architectures. However, their performances do not at present reach the values required for an optimum system. We are therefore studying new MOEMS-based MDM architectures in close collaboration with opto-electronics research laboratories, and we plan to realize first test devices by the middle of next year.

4.4.4.4. References

T. G. Bifano, R. K. Mali, J. K. Dorton, J. Perreault, N. Vandelli, M. N. Horenstein and D. A. Castanon, "Continuous-membrane surface-micromachined silicon deformable mirror", *Opt. Eng.*, **36** (5), pp. 1354-1360 (1997).

R. Burg, P.Y. Bely, B. Woodruff, J. MacKenty, M. Stiavelli, S. Casertano, C. McCreight and A. Hoffman, "Yardstick integrated science instrument module concept for NGST", in *Space Telescopes and Instruments V*, P. Y. Bely, J. B. Breckinridge, ed., SPIE **3356**, 98-105 **(**1998).

D. Burgarella, V. Buat, K. Dohlen, F. Zamkotsian and P. Mottier, "Multi-object spectroscopy in space", in *Proceedings of the 34th Liege International Astrophysics Colloquium (International Workshop on the Next Generation Space Telescope "Science drivers and technological challenges")*, Liege, Belgium (June 1998).

W. D. Cowan, M. K. Lee, B. M. Welsh, V. M. Bright and M. C. Roggeman, "Optical phase modulation using a refractive lenslet array and microelectromechanical deformable mirror", *Opt. Eng.* **37** (12), pp. 3237-3247 (1998).

K. Dohlen, M. Saisse, G. Clayesen, P. Lamy, J-L. Boit, "Optical designs for the Rosetta narrow-angle camera", *Opt. Eng.* **35**, pp. 1150-1157 (1996).

L. M. Foucault, "Mémoire sur la construction des télescopes en verre argenté", *Ann. Obs. Imp. Paris* **5**, p. 197 (1859).

Larry J. Hornbeck, "Digital light processing and MEMS: timely convergence for a bright future", in *Micromachining and Microfabrication Process Technology*, K. W. Markus, ed., Proc. SPIE **2639**, pp. 2-2 (1995). Color reprint available from Texas Instruments Digital Imaging Group.

L. Mertz, "Concentric spectrographs", *Appl. Opt.* **16**, 3122-3124 (1977).

A. Offner, "New concepts in projection mask aligners", *Opt. Eng.* **14**, 130-132 (1974).

J. A. Perreault, T. G. Bifano and B. M. Levine, "Adaptive optic correction using silicon based deformable mirror", in *Proceedings of the SPIE conference on High-Resolution Wavefront Control*, SPIE **3760**, 12-22, Denver, USA (1999).

M. C. Roggeman, V. M. Bright, B. M. Welsh, S. R. Hick, P. C. Roberts, W. D. Cowan and J. H. Comtois, "Use of micro-electro-mechanical deformable mirrors to control aberrations in optical systems: theoretical and experimental results", *Opt. Eng.*, **36** (5), pp. 1326-1338 (1997).

G. Vdovin, S. Middelhoek and P. M. Sarro, "Technology and applications of micromachined silicon adaptive mirrors", *Opt. Eng.*, **36** (5), pp. 1382-1390 (1997).

F. Zamkotsian, K. Dohlen, P. Lanzoni, S. Mazzanti, M. Michel, V. Buat, D. Burgarella, "Knife-edge test for characterization of sub-nanometer deformations in micro-optical surfaces", in *proceedings of 44th SPIE's Annual Meeting on Optical Science, Engineering, and Instrumentation*, Proc. SPIE **3782**, Denver, USA (July 1999).

F. Zamkotsian, K. Dohlen, D. Burgarella, V. Buat, "Aspects of MMA for MOS : optical modeling and surface characterization, spectrograph optical design", in *proceedings of NASA colloquium on NGST Science and Technology Exposition*, ASP Conf. Ser. **207**, pp. 218-224, Hyannis, USA (September 1999).

F. Zamkotsian and K. Dohlen, "Surface characterization of micro-optical components by Foucault's knife-edge method: the case of a micro-mirror array", *Applied Optics* **38**, pp. 6532-6539 (November 1999).

F. Zamkotsian, K. Dohlen, M. Ferrari, "Micro-deformable mirror for adaptive optical systems on extremely large telescopes", in *proceedings of SPIE conference on Astronomical Telescopes and Instrumentation 2000*, Proc. SPIE **4007**, pp. 547-554, Munich, Germany (March 2000).

F. Zamkotsian, K. Dohlen, V. Buat, D. Burgarella, "Multi-Mirror Array Unit-Magnification Multi-Object Spectrograph for NGST", in *proceedings of SPIE conference on Astronomical Telescopes and Instrumentation 2000*, Proc. SPIE **4013**, pp. 580-586, Munich, Germany (March 2000).

5. Management

5.1.1. Telescope study group

5.1.1.1. Scientific consortium

Science Team	
Chantal Balkowski	Observatoire de Paris-Meudon
Pierre Barge	Laboratoire d'Astrophysique de Marseille
Alain Blanchard	Observatoire Midi – Pyrénées
Véronique Buat	Laboratoire d'Astrophysique de Marseille
Denis Burgarella (P.I.)	Laboratoire d'Astrophysique de Marseille
Véronique Cayatte	Observatoire de Paris-Meudon
Françoise Combes	Observatoire de Paris-Meudon
Magali Deleuil	Laboratoire d'Astrophysique de Marseille
Kjetil Dohlen	Laboratoire d'Astrophysique de Marseille
Marc Ferrari	Laboratoire d'Astrophysique de Marseille
Jean Gay	Observation de la Côte d'Azur
Brett Gladman	Observatoire de la Côte d'Azur
François Hammer	Observatoire de Paris-Meudon
Ariane Lançon	Observatoire de Strasbourg
Vincent Le Brun	Laboratoire d'Astrophysique de Marseille
Jean-François Leborgne	Observatoire Midi-Pyrénées
Michel Marcelin	Laboratoire d'Astrophysique de Marseille
Alain Mazure	Laboratoire d'Astrophysique de Marseille
Claire Moutou	Laboratoire d'Astrophysique de Marseille
Bruno Milliard	Laboratoire d'Astrophysique de Marseille
Patrick Petitjean	Institut d'Astrophysique de Paris
Yves Rabbia	Observatoire de la Côte d'Azur
François Rigaud	Observatoire de Paris-Meudon
Annie Robin	Observatoire de Besançon
Fréderic Sayede	Observatoire de Paris-Meudon
Daniel Schaerer	Observatoire Midi-Pyrénées
Jean Schneider	Observatoire Paris-Meudon
François Thévenin	Observatoire de la Côte d'Azur
Farrokh Vakili	Observatoire de la Cote d'Azur
David Valls-Gabaud	Observatoire Midi –Pyrénées
Christian Veillet	Canada-France-Hawaii Telescope
Frédéric Zamkotsian	Laboratoire d'Astrophysique de Marseille

5.1.1.2. Industrial constellation

Concerning the realization of large astronomical telescopes, a high industrial expertise already exists in Europe as demonstrated with the achievement of the 8-10 m class telescope projects (VLT, Gemini, Grantecan). SAGEM–Reosc has world leadership in large optics manufacturing, and we are working closely with that company for our study. Their remarkable expertise in manufacturing 8-m optics perfectly complements the proposed concept using 6-8 m segments.

Many European mechanics companies have also been involved in the recent large telescope projects. The Belgian AMOS proposed a detailed design for the VLT Unit Telescopes, and ha s been selected to build the VLT Auxiliary Telescopes. This company is associated to the NG-CFHT study, and will perform mechanical and thermal studies during phase 2.

For some key technologies, such as adaptive structures and micro-optics, the needed expertise already exists in France and in Europe. Adaptive structure concepts have already been developed for space based and military projects, and large consortia of the European space industry are well advanced in this domain. Another key component for segmented telescopes is the high-accuracy magneto-mechanical sensor for segment phasing. The French company FOGALE is well placed in the field of non-contact sensor technologies, and participate in the VLTI project. Micro-optics is still mainly a research field, but its industrial development is quickly evolving. We are currently working in close collaboration with LAAS, a major micro-technology research laboratory in France.

5.1.2. ROM cost

A preliminary ROM cost, based on the Grundmann report (1997), has been established, leading to a total cost estimation of 120 millions dollars, excluding instruments. For a total envelope of 200 M$, this leaves 80 M$ for a first-light instrument suit. The cost estimate is compared with the old CFH facility and other existing large telescope projects in Table 1. One can notice that the cost evolution is roughly proportional to aperture diameter, while the scientific output is roughly proportional to aperture area. This is commonly expressed in terms of the *cost index* ($/d²), which decreases with increasing telescope size.

Telescope	**CFHT**	**Gemini**	**Keck I**	**NG-CFHT**
Period	1973-1979	1992-1998	1986-1992	2002-2010
Cost (M$)	27	87.5	63.5	117

Table 1: NG-CFHT cost comparison with other large telescope and historical CFHT

An estimated cost for a 20 m NG-CFHT has been obtained by extrapolating the estimations made by Grundmann (1997) for an 8 to 12 m facility (Table 2). The total cost is a function of the mirror diameter and not the surface, which allows the budget per collecting area (cost index) of a 20-m to be half that of a 10-m telescope.

Telescope diameter	**8 m**	**10 m**	**12 m**	**16 m**	**20 m**
Design & Management	8	8	8	8	8
Mirror Blanks	3	5	9	12	15
Mirror Polishing	6	10	16	24	32
Manufacture - Telescope	7	7	8	10	12
Site Preparation	2	2	2	2	2
Enclosure	9	9	11	15	20
Erection/Running in	4	4	4	5	5
Mirror Active Control	6	7	7	10	12
Mirror Passive Control	3	4	4	5	6
Software-Hardware Controls	5	5	5	5	5
Total (no instruments)	**53**	**61**	**74**	**96**	**117**
Cost index ($/d²)	.83	.61	.51	0.38	0.29

Table 2. NG-CFHT cost comparison for different telescope size (M$). The total cost of a 20-m telescope, without instrumentation, fits in a 120 M$ envelope. Cost estimations for 8- to 12-m telescopes have been extracted from Grundmann, 1997, "Report on Option for use of the Existing Pier with a New Telescope".

Figure 35 shows a graphical representation of the cost estimates. Mirror manufacturing includes both blank and polishing, structure and control include both structure, active and passive control and software as well as running in cost. It is interesting to note that the cost of mirror manufacture grows more quickly than the other posts and becomes the main cost driver for telescopes larger than about 16 m.

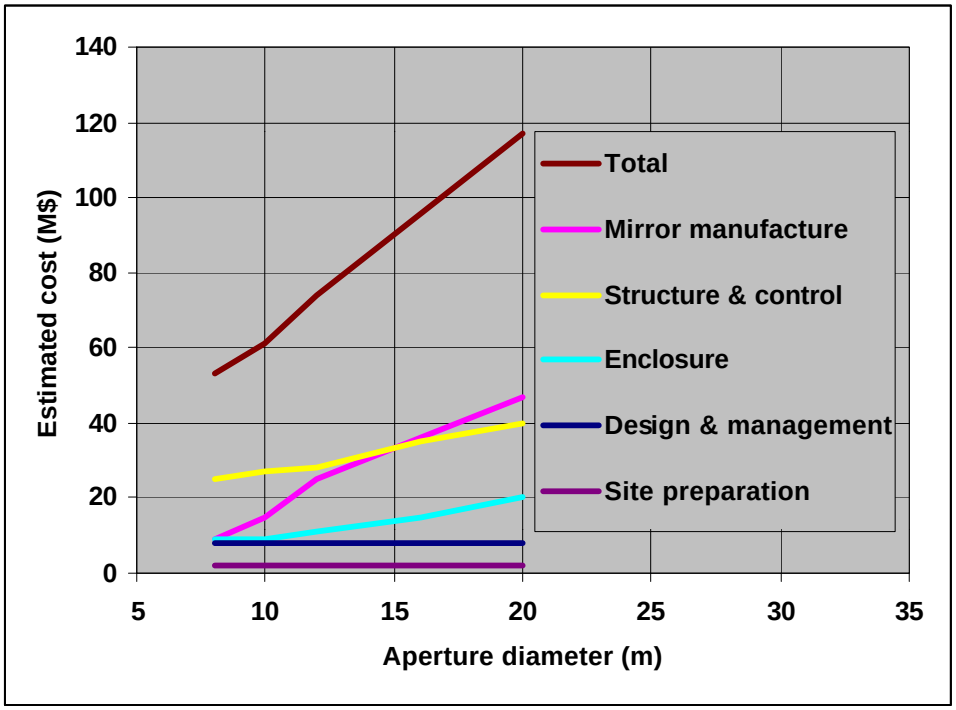

Fig. 35: Comparison of the cost of optics, structure, enclosure, design, and site preparation as function of telescope aperture. Estimations based on the Grundmann report.

5.1.3. Planning

A tentative planning has been made, indicating first scientific light by the end of 2009. The planning assumes project funding from January 2002. The main drivers for the planning are structural design and optical fabrication. These items are closely linked, and it is risky to freeze the optical design and blank specifications before the mechanical design is well defined. We have reserved two years for this work, allowing the four years of optical fabrication to start in 2004.

Operation of the old telescope may be continued until the beginning of 2005. At that point, the old telescope must be dismantled in order to allow building works on the new dome to start in 2006. The blind period is 3.5 years before first engineering light by the end of 2008.

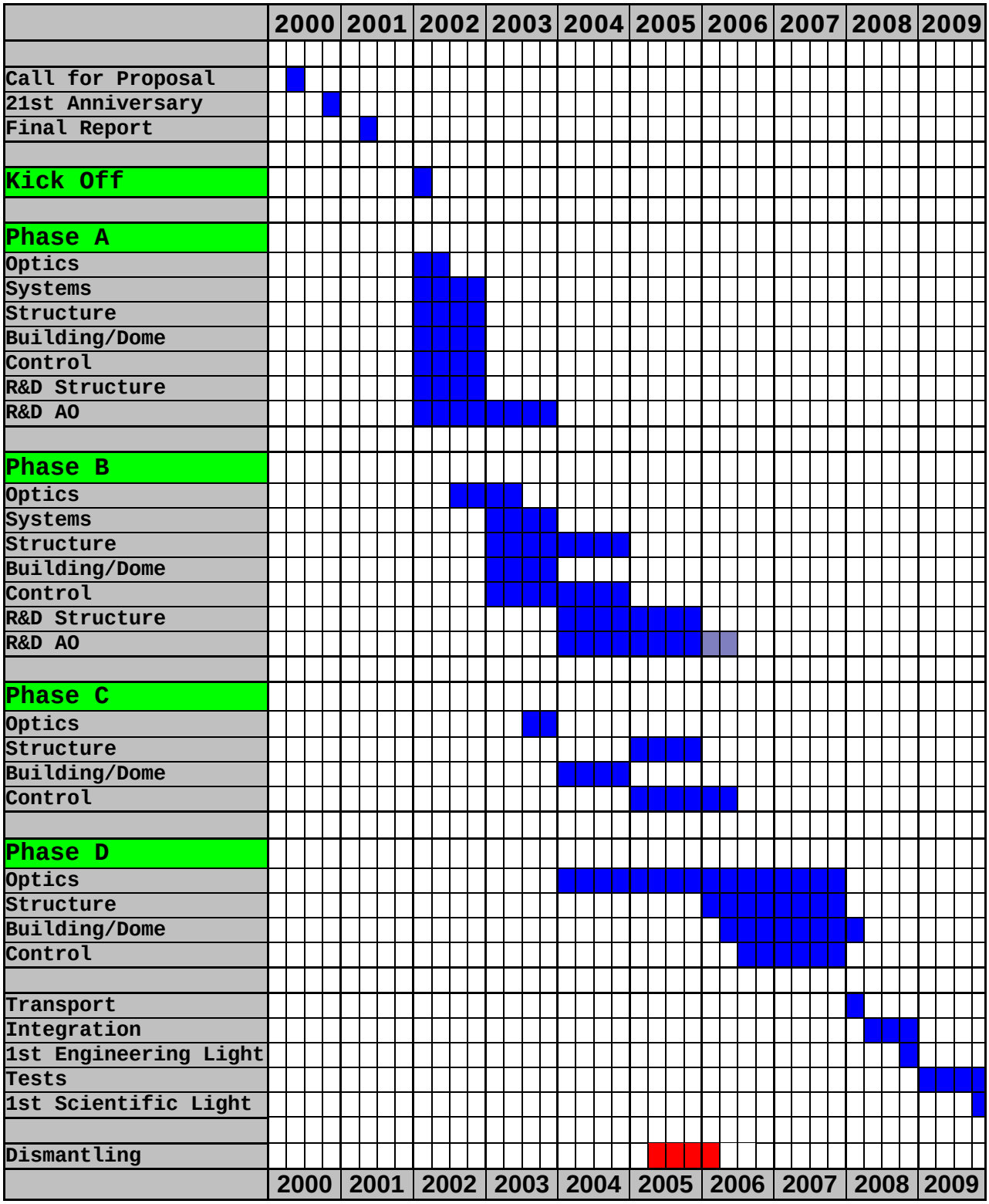
2000
2001
2002
2003
2004
2005
2006
2007
2008
2009
Call for Proposal
21st Anniversary
Final Report
Kick Off
Phase A
Optics
Systems
Structure
Building/Dome
Control
R&D Structure
R&D AO
Phase B
Optics
Systems
Structure
Building/Dome
Control
R&D Structure
R&D AO
Phase C
Optics
Structure
Building/Dome
Control
Phase D
Optics
Structure
Building/Dome
Control
Transport
Integration
1st Engineering Light
Tests
1st Scientific Light
Dismantling
2000
2001
2002
2003
2004
2005
2006
2007
2008
2009

6. Appendix: REOSC-SAGEM report

SAGEM/REOSC optical fabrication feasibility study